June 10 - Annual Muri Review

Gerry Lucovsky, Prinicipal Investigator
NC State University

RA Students: Hyungtak Seo and Joseph P Long (graduated), JinWu Kim and Daniel Zeller

Post Docs: Kwun-Bum Chung, Leonardo Miotti, Karen Baz Pastos

Len Feldman, Presenter
Rutgers University and Vanderbilt University

Additional Support: NSF, SRC and DTRA

outline

i) mono- and di-vacancy defects in HfO_2

ii) monoclinic HfO_2 and HfSiON on Ge

objective - provide a science base for optimization
of HfO_2 and Hi Si oxynitride dielectrics
for survivable devices, rad hard on Si and Ge substrates

X-ray absorption and photoemission spectroscopies, XAS and SXPS,

conduction and valence band electronic states

band edge, intrinsic and chemical defects

defects, and dependence on processing are then compared with defects, traps and fixed charge, detected electrically

relationship to

CMOS

(i) define and narrow the field of high-k dielectrics that meet the aggressive scaling required deep sub-micron- and nano-CMOS, and
(ii) identify processing constraints that apply to Ge and Si substrates

rad testing

(i) differences in rad hardness/survivability of generically similar dielectrics
HfO_2 and Hf Si oxynitride on Si and Ge substrates and correlations with

DEFECTS IN DIELECTRICS

1. Why do we care? Leakage paths, breakdown points, trapping centers in radiation damage. Mostly oxygen vacancies

2. Nature of defects----intrinsic or processing dependent ?

3. Vacancies are hard to "see"---positrons, energetic electron displacement, material contraction. This work-x-ray, electron spectroscopy!

4. Oxygen vacancies plague all of the current oxide work!

H 1																	He 2
Li 3	Be 4											B 5	C 6	N 7	O 8	F 9	Ne 10
Na 11	Mg 12											Al 13	Si 14	P 15	S 16	Cl 17	Ar 18
K 19	Ca 20	Sc 21	Ti 22	V 23	Cr 24	Mn 25	Fe 26	Co 27	Ni 28	Cu 29	Zn 30	Ga 31	Ge 32	As 33	Se 34	Br 35	Kr 36
Rb 37	Sr 38	Y 39	Zr 40	Nb 41	Mo 42	Tc 43	Ru 44	Rh 45	Pd 46	Ag 47	Cd 48	In 49	Sn 50	Sb 51	Te 52	I 53	Xe 54
Cs 55	Ba 56	Lu 71	Hf 72	Ta 73	W 74	Re 75	Os 76	Ir 77	Pt 78	Au 79	Hg 80	Tl 81	Pb 82	Bi 83	Po 84	At 85	Rn 86
Fr 87	Ra 88	Lr 103	Db 104	Jl 105	Rf 106	Bh 107	Hn 108	Mt 109	110	111	112	113	114	115	116	117	118

La 57	Ce 58	Pr 59	Nd 60	Pm 61	Sm 62	Eu 63	Gd 64	Tb 65	Dy 66	Ho 67	Er 68	Tm 69	Yb 70
Ac 89	Th 90	Pa 91	U 92	Np 93	Pu 94	Am 95	Cm 96	Bk 97	Cf 98	Es 99	Fm 100	Md 101	No 102

22 Ti titanium : [Ar] $3d^2$ $4s^2$

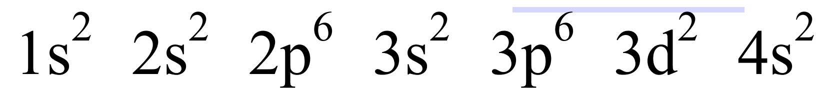

72 Hf hafnium : [Xe] $4f^{14}$ $5d^2$ $6s^2$

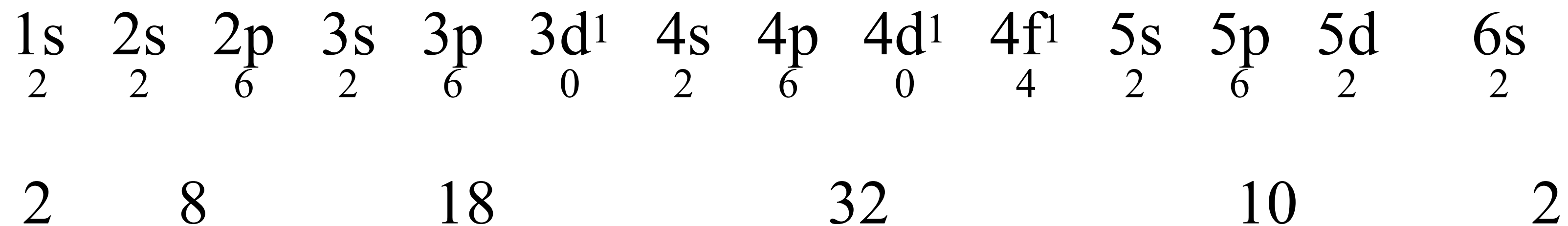

...erate, E_g, groups as determined by the coordination and local symmetry of th... ...s with respect to their O-atom neighbors, and then (2) the removal of these two ...efold degeneracies by Jahn–Teller (J–T) bonding distortions that are accompani... ...metry reductions at the TM atom bonding sites [12,20]. See Figure 10.1 for a sche...

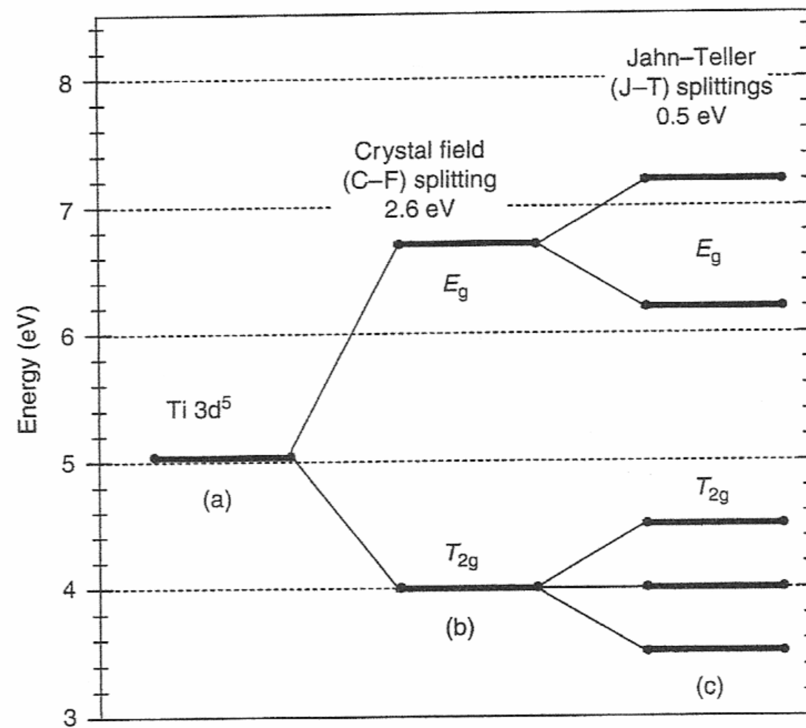

...URE 10.1
...ematic representation of C–F and Jahn–Teller splittings for Ti relative to the fivefold degenerate ... state: (a) the atomic Ti 3d state; (b) in an ideal octahedral field; and (c) in a distorted octahedral fie... ...rgy scale is arbitrary, i.e., the energy of the triply degenerate T_{2g} state has been set to 4 eV.

electronic structure of transition metal oxides - FA Cotton

bonding and anti-bonding states - symmetry adopted linear combinations of atomic states/symmetries of constituent atoms

ionic model

valence band occupied O 2p σ and π conduction band empty states Ti 3d 4s, 4p for 6-fold coordination TiO_2 empty states Hf 5d 6s, 6p, 5f for 7/8-fold coordination HfO_2

conduction band empty states not restricted to atomic valence state

valence states - O^{2-} O $2s^2$, $2p^2$

Ti^{4+} Ti $3s^2$,$3p^6$ d^0 configuration, no occupied d-states

Hf^{4+} Hf $5s^2$,$5p^6$ d^0 configuration, no occupied d-states

partially ionic model

bonding and anti-bonding states - symmetry adopted linear combinations of atomic states/symmetries of constituent atoms

valence-conduction band transitions - O 2p - O 2p*, each mixed with either Ti or Hf states

schematic molecular orbital diagram for TiO_2

6 fold-coordinated Ti^{4+} ions, and 3 fold-coordinated O^{2-} ions

covalent mixing of Ti and O atomic states in symmetry adapted molecular orbital states, SALCs - FA Cotton, 1962

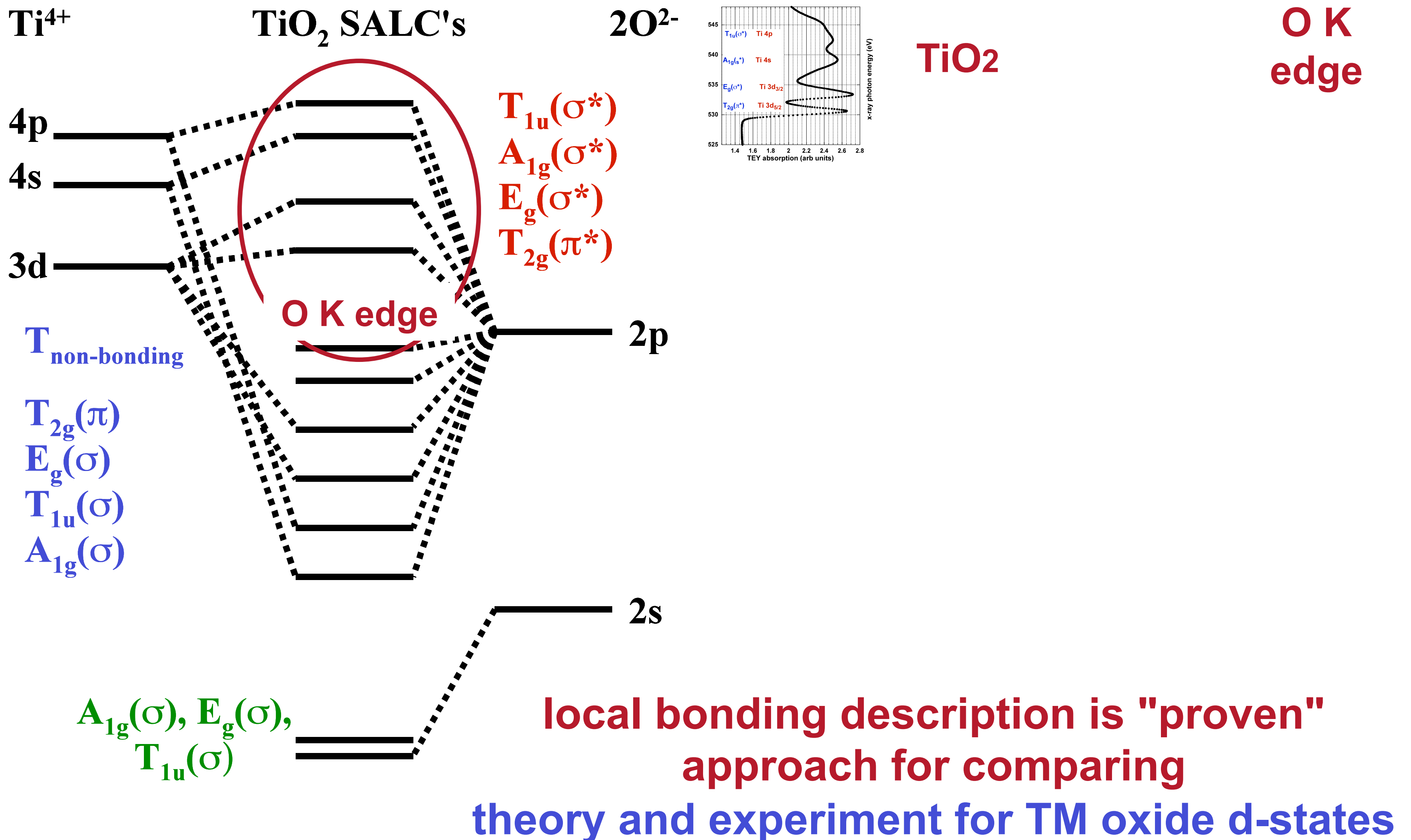

schematic representation of local bonding in monovacancies and divacancies

(a) mono-vacancy defect in TiO_2

(b) monovacancy defect in HfO_2

3 fold coordinated O

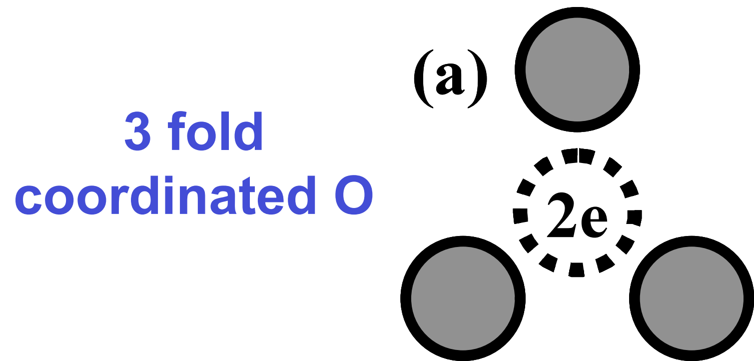

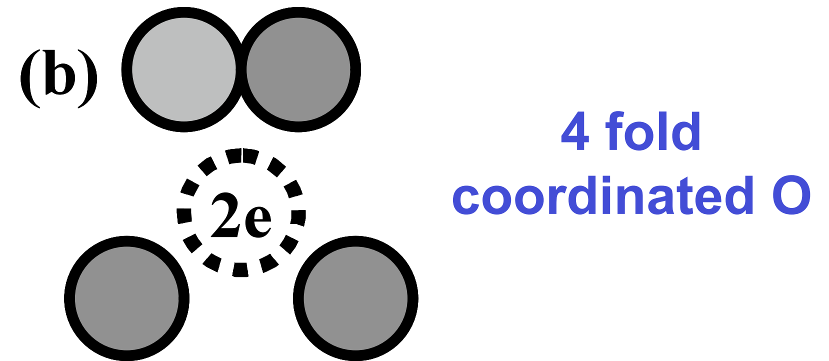

4 fold coordinated O

equivalent to two edge connected tetrahedra

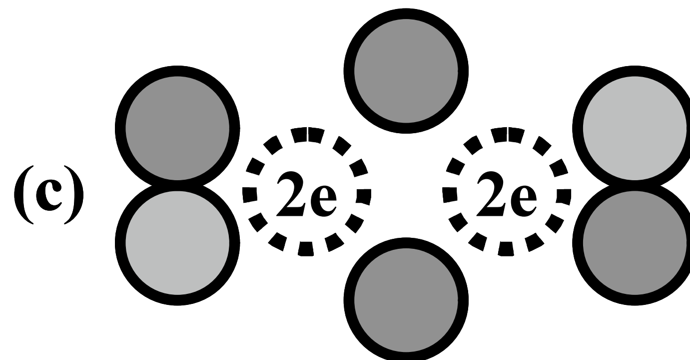

distorted octahedron with 4 electrons

(c) divacancy defect in HfO_2

theory-supported model for vacancy defects

charge neutrality each O-atom - replaced by 2 electrons

Robertson/Shluger distribute these electrons over

d-states of all nearest-neighbor Hf or Ti atoms:

theory - d-states, not contributing to bonding, are *occupied digitally*

d^n representation - n is the number of d-electrons

not contributing to bonding

determined by formal valence of TM in ionic model

HfO_2 Hf atom valence electrons - $6s^25d^2$

TiO_2 Ti atom valence electrons - $4s^23d^2$

Hf^{4+}, Ti^{4+} are d^0 after 4 electrons are removed

no occupied states above VB edge

defect states - equivalent to pairs of T^{3+} - $4s^23d^1$

with one occupied d-state - $2d^1$ or $1d^2$

(mono)-vacancy defects for TiO_2 are d^2

2 occupied states at valence band edge

divacancy defects for HfO_2 are d^4

defect states for d^2 "fit" into band gap: TiO2

E_{gap} = 3.1 eV >Δ(C-F) = 2.6±0.1eV

HfO2 E_{gap} = 5.7 eV >Δ(C-F) = 3.6±0.2eV

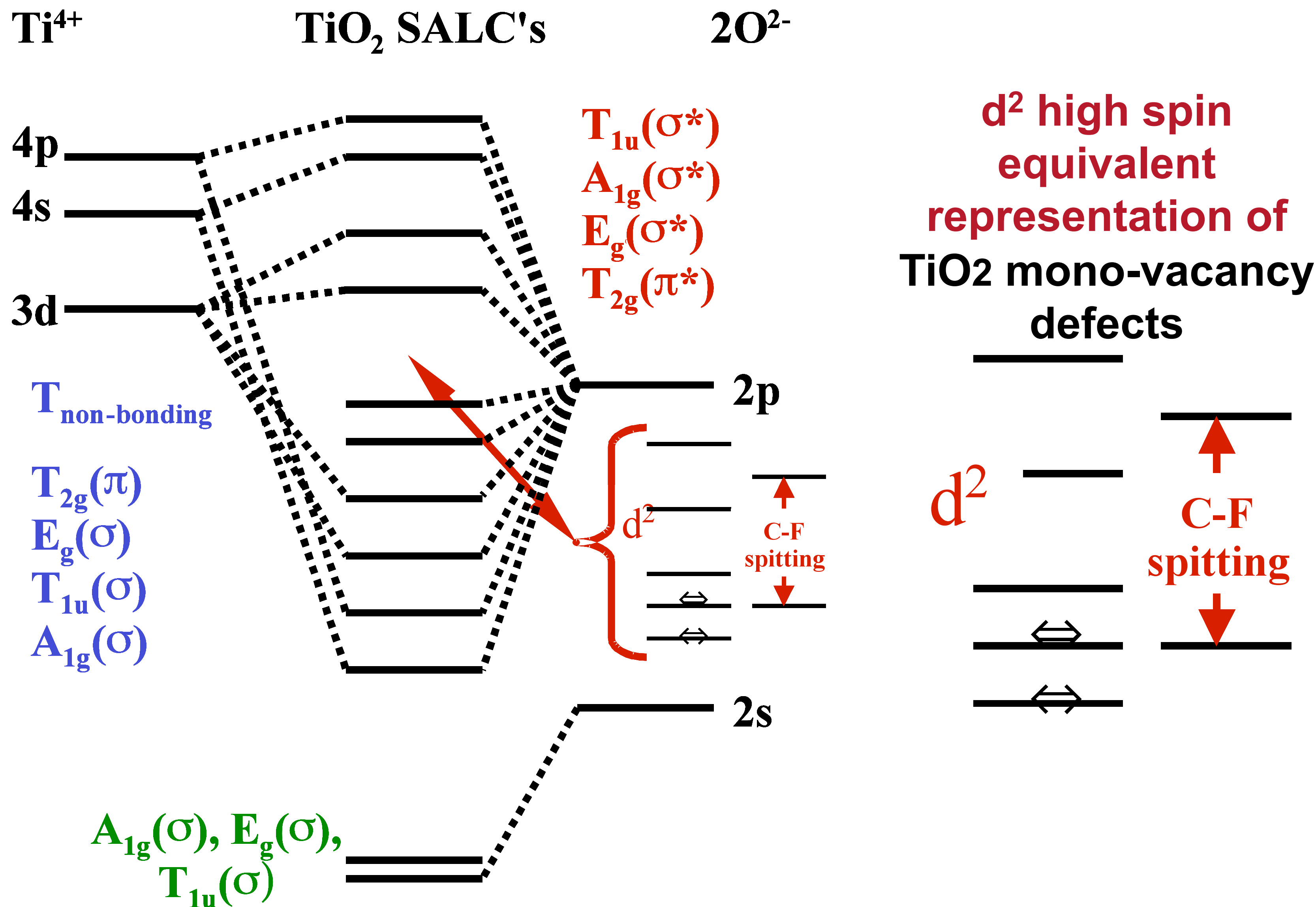

Micro-structure of nano-crystalline HfO_2 and non-crystalline Hf silicates and nitrided Hf silicates

nano-crystalline HfO_2

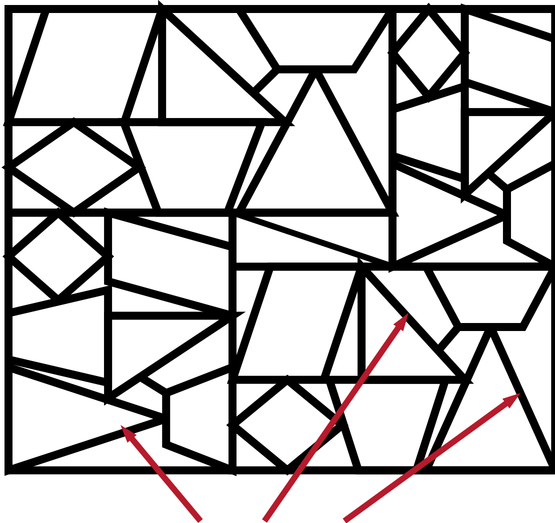

grain boundaries

crystallite size: 2 to 100 nn

grain boundaries - intrinsic bonding defects

local defects at band edges

trap both holes and electrons

amorphous Hf silicate

isotropic and homogeneous

no discernable granularity

band tail states due to random local atomic structure

localized defect states

generally deep in gap

specific bonding defects

broken bonds - chemical impurities

Spectroscopic evidence for band edge defects in HfO_2

Soft x-ray photoelectron spectroscopy (SXPS)

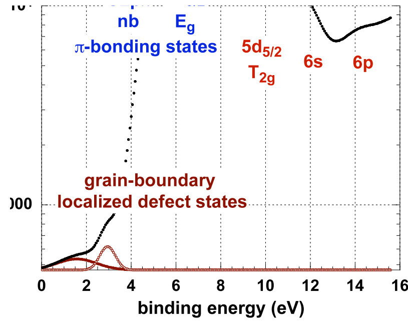

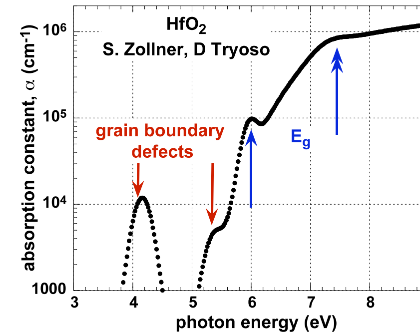

partially-filled defect states at valence band edge

hole or electron traps

empty defect states at conduction band edge

electron traps

intrinsic defects in elemental and complex TM oxides have occupied valence band edge states

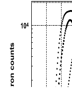

rules out Robertson and Shluger mono-vacancies models

K. Xiong, J. Robertson, S.J. Clark, APL 87 (2005)

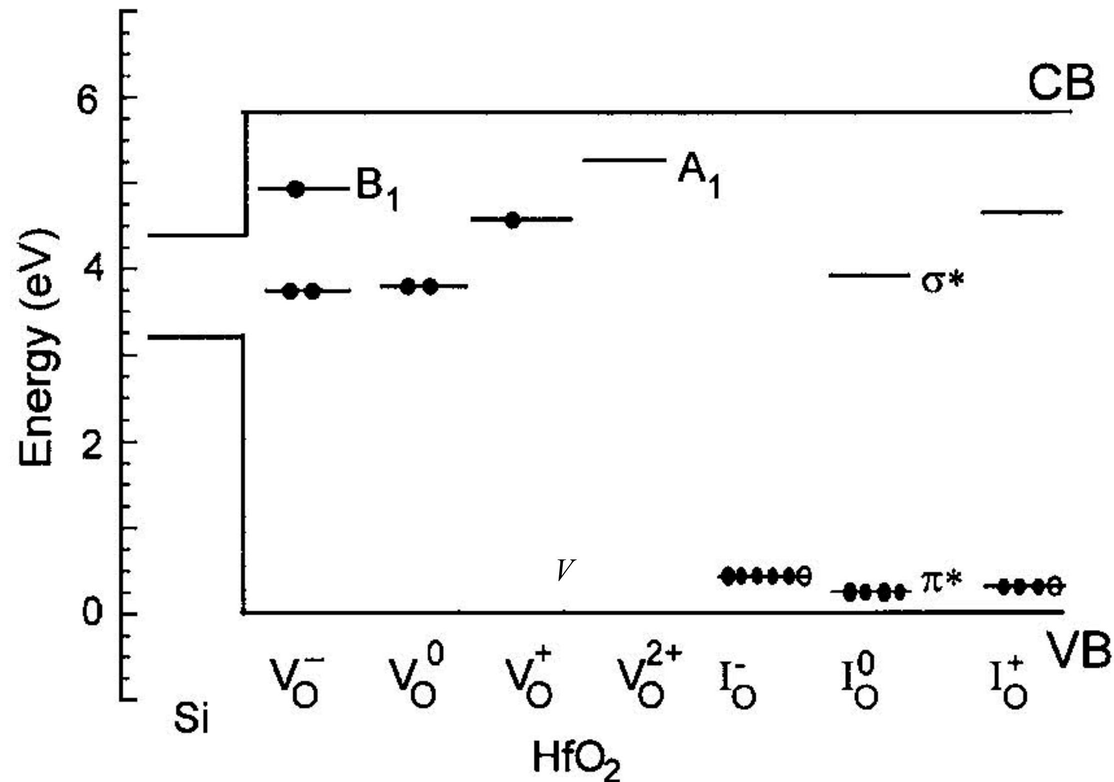

FIG. 2. Summary of calculated energy levels of the relaxed O vacancy and interstitial, in their various charge states.

$[V_o]^-$ and $[V_o]^0$ are the intrinsic bonding defects

Robertson suggests are identified spectroscopically and in electrical measurements, but does not explain valence band edge defects

intrinsic defects in elemental and complex TM oxides are O-atom vacancies

two issues -- (i) single atom vacancies - mono-vacancies, or double atom vacancies di-vacancies as in c-Si

(ii) mobile, or fixed or immobile

both resolved spectroscopically

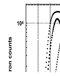

occupied defects at valence band edge

rules out Robertson and Shluger mono-vacancies models

defect density is a function of film thickness - correlates with splitting of E_g d-state feature

larger grains in 4 nm thick film- defect density 10x higher than 2 nm thick film

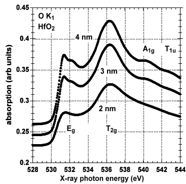

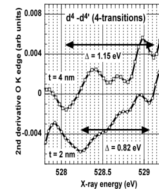

fewer and qualitatively different defects in 2 nm film

mobile defects less effective in holding charge than immobile defects

energy level diagram for occupied and empty defects states:
(left) spectroscopic energies referenced to valence band edge, WRONG!
(right) empty state energies referenced to d-d'transitions from occupied states above valence band

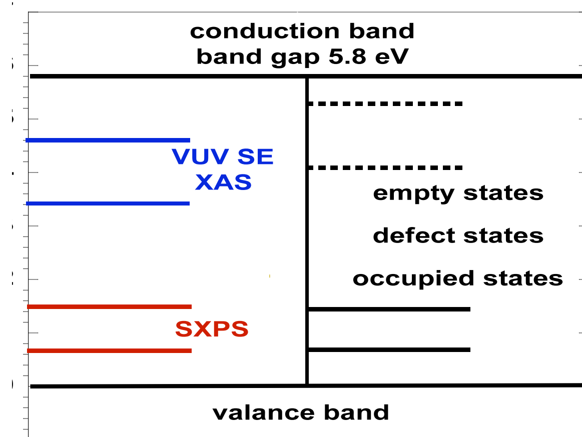

differences in J-V correlate with differences in conduction band edge defect states

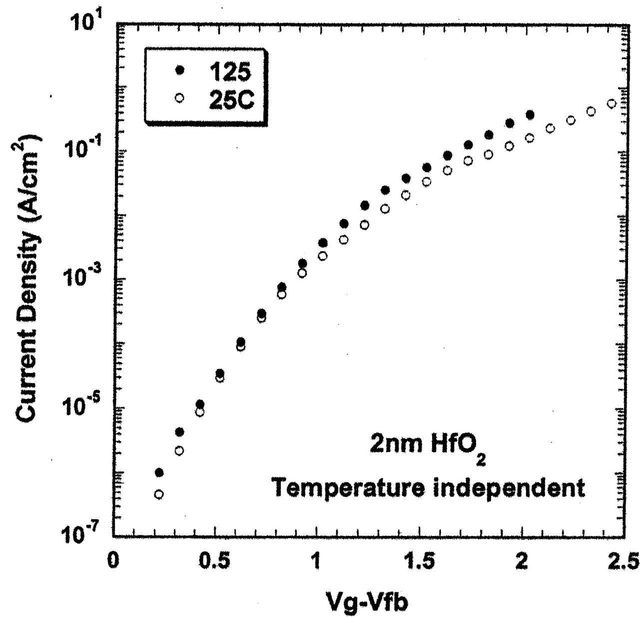

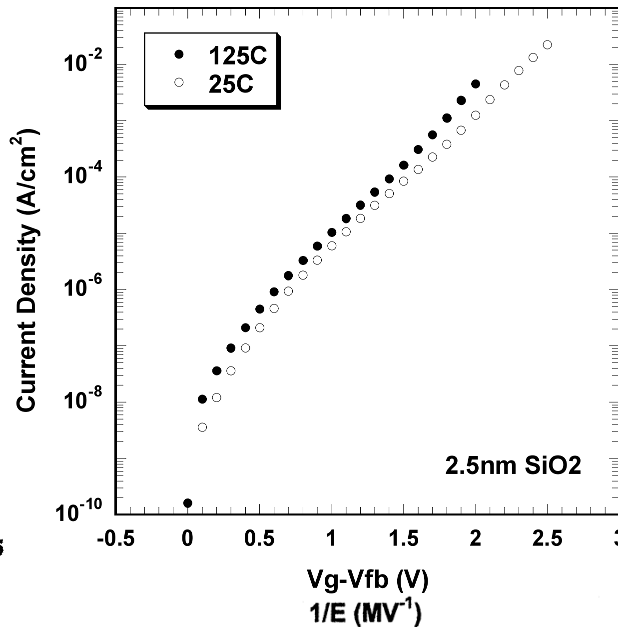

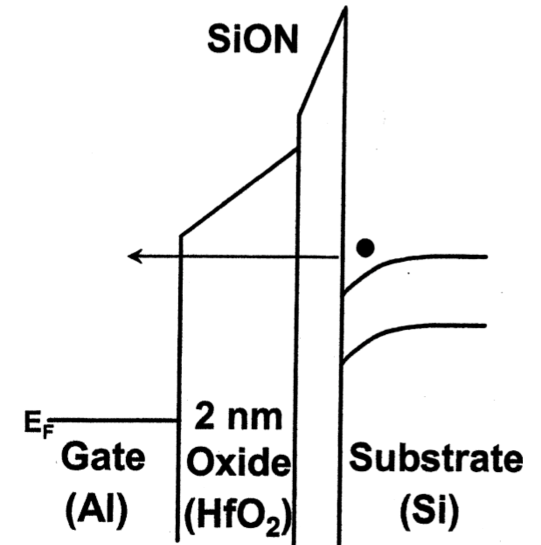

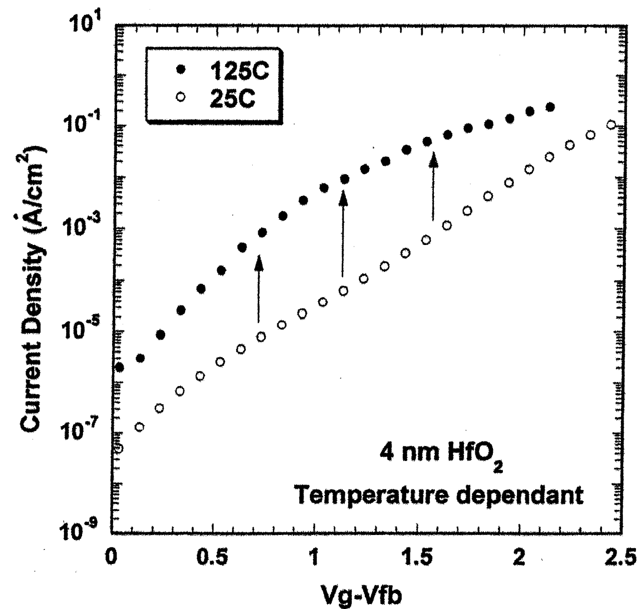

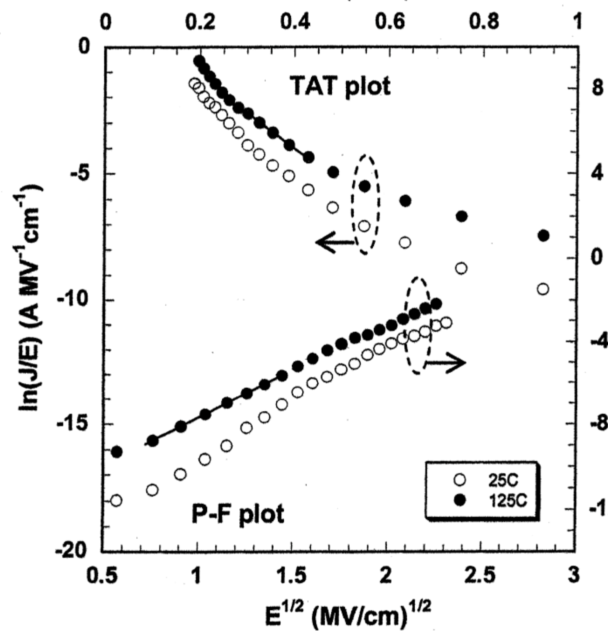

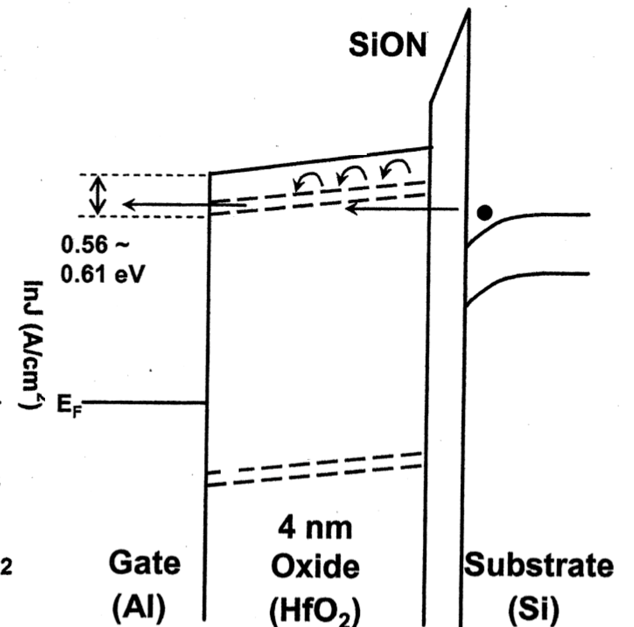

- **removal of Ge dielectrics between Ge and HfO_2**

textured epitaxial alignment between HfO_2 and Ge(001)

- **old clean - acidic -- Hf/H_2O 6 cycles - 'thick' GeO_2**
- **new clean - neutral/basic - 'thinner' GeO_2**
- **electrical results**

dielectrics on Ge a “devious” pathway to eliminate Ge-O and Ge-N bonding

surface nitridation
GeOx - plasma or chemical
Ge (001) substrate

pre-deposition Ge passivation
to prevent active plasma O/Hf/Ti
from reacting with
at Ge surface during deposition

remote plasma HfO_2/TiO_2
surface nitridation
GeOx - plasma or chemical
Ge (001) substrate

remote plasma deposition of
HfO_2/TiO_2 at 300°C

Ge passivation
prevents active plasma O/Hf/Ti
from reacting with
at Ge surface during deposition

chemical = pre-deposition cleans

- old clean - acidic -- Hf/H_2O 6 cycles - ‘thick’ GeO_2
- new clean - neutral/basic - ‘thinner’ GeO_2

post deposition annealing in Ar ambient

(i) two step 550°C / 800°C or (ii) single step 800°C

remote plasma HfO_2/TiO_2
nano-grain growth - textured film
epi-regrowth Ge
Ge (001) substrate

Ge-O sublimes ~400-500°C
Ge-N decomposes ~600-650°C

solid phase epi-regrowth of Ge on Ge substrate

nano-grain "reorganization" textured films with "c-axis" aligned relative to dimer rows of Ge substrate

we will focus on two aspects of this process

i) verification of process variations that result in HfO_2 and HfSiON in "direct contact" with Ge(0001); i.e., no detectable Ge dielectrics forming an interfacial transition region

ii) relationship between processing and defects extracted from MOSCAP test devices

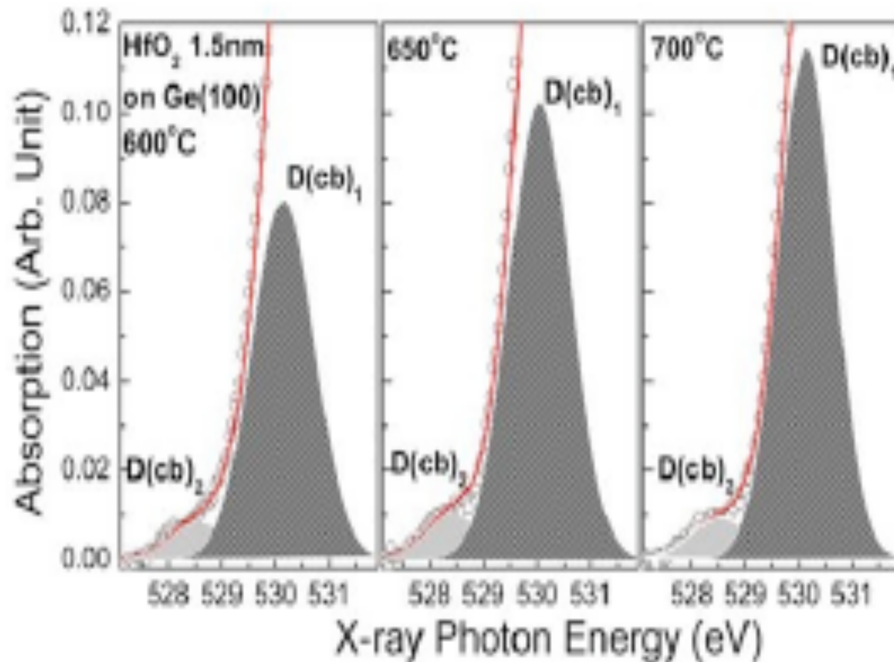

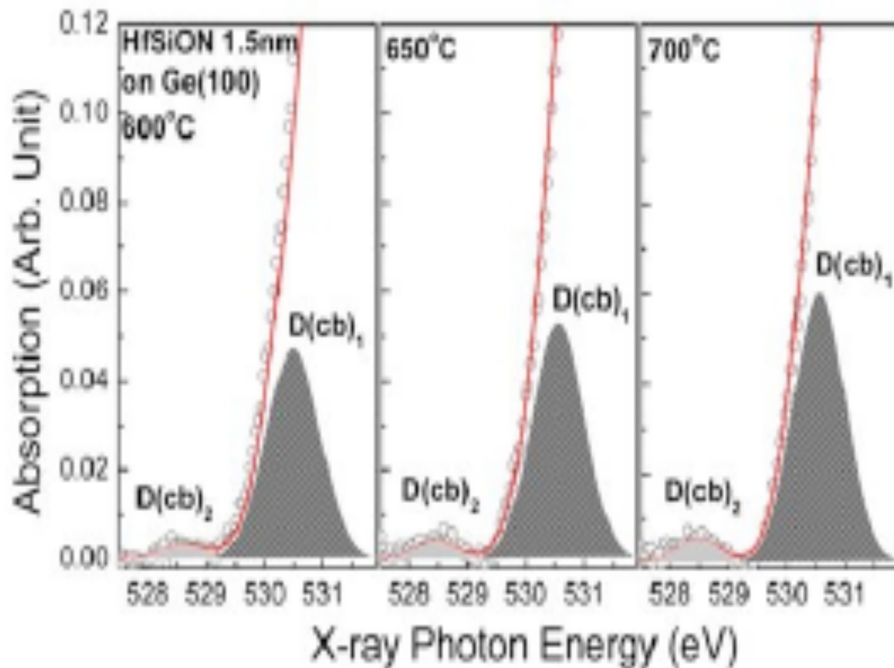

(a) Thermal evolution of the O K_1 spectra for both HfO2 and HfSiON over a narrow energy region

\below the doubly-degenerate Hf 5d conduction band edge states as a function of PDA temperature.

two deconvoluted peaks, labeled $D(cb)_1$ and $D(cb)_2$, indicate the defect states determined by Gaussian fits of the XAS O K_1 edge spectra.

lower density of defects by spectroscopy for HfSiON than HfO2 - confirmed by CV

Capacitance-voltage (CV) for *n*-MOSCAPS 5nm HfSiON on *n*-type Ge (100): normalized by C/Cox, as a function of PDA temperature-arrows indicate clockwise hysteresis loop.

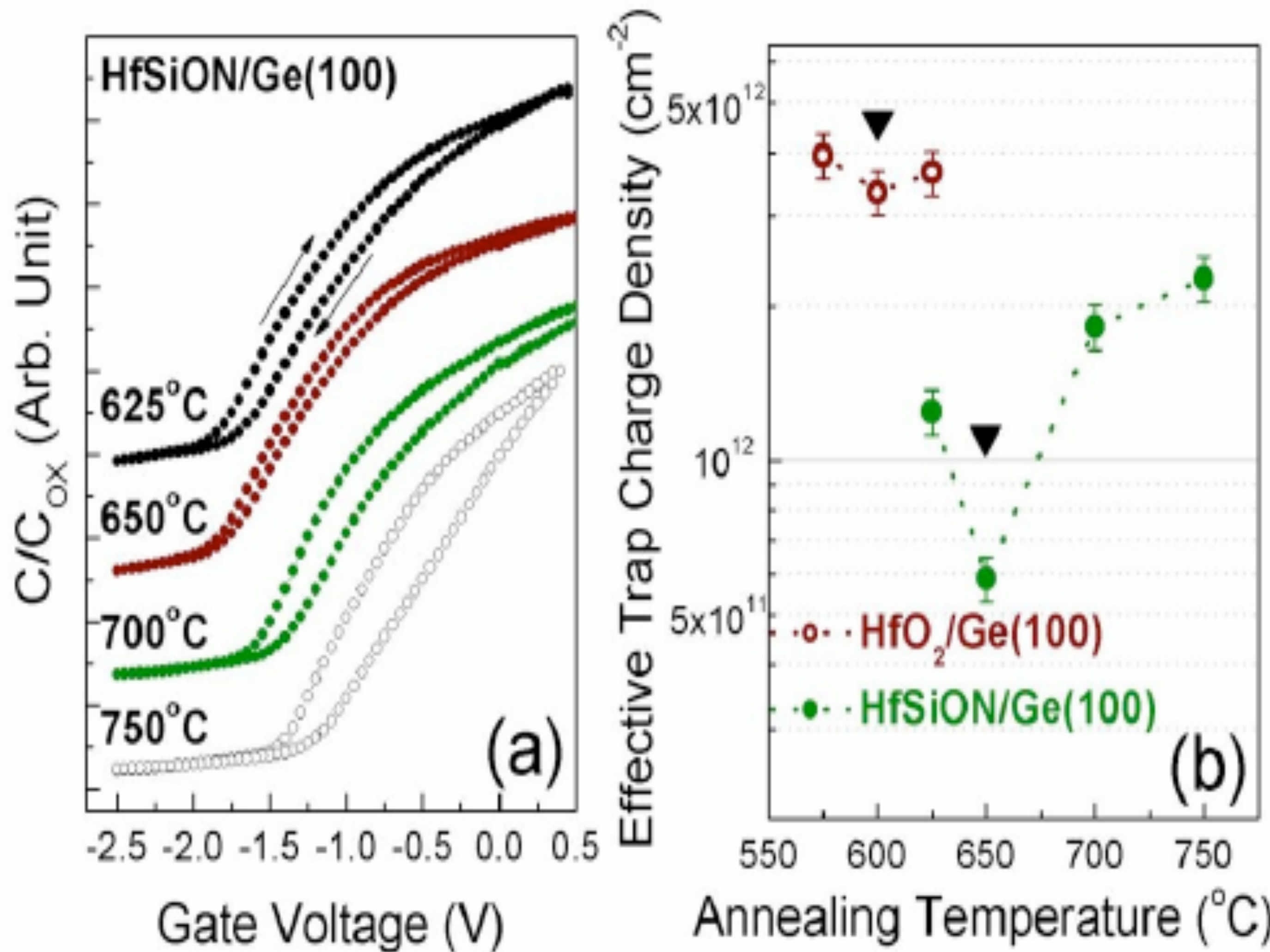

lowest trap density same as Saraswat's (Stanford Univ) best

HfSiON on Si - X-ray stress similar to SiO_2 no negative fixed charge as in HfO_2

defects lower than in HfO_2 agree with XAS

conclusions with respect to

CMOS

(i) HfO_2 and Hf Si oxynitride on Si: there is a direct correlation between intrinsic bonding defects observed in spectrsocopic studies with those obtained in electrical measurements on MOSCAPs

(i) HfO_2 and Hf Si oxynitride on Ge: due to limitations on processing temperatures, generally lower than 800C, often more restrictive to 650C, CMOS applications are generally more limited

currently been pursued

rad testing

CMOS - first important result under DTRA

radiation induced defects can be observed spectroscopically in XAS, spectroscopic ellipsometry and cathodoluminescence spectroscopy

plans for next year

(i) prepare MOSCAPs on Ge(100) and Si/SiON/ substrates for rad testing using optimized Hf Si Oxynitride composition $(HfO_2)_{0.3}(SiO_2)_{0.3}(Si_3N_4)_{0.4}$

(ii) fabricate stacked HfO_2/HfSiON on Ge(100) MOSCAPs using the HfSiON as a thin interfacial transition and compare electricals with HfO_2 and HfSiON on Ge(100) determine defect concentrations, and electrical stress induced defects

(iii) Based on results from (ii) prepare another set of MOSCAPs for rad testing and compare defects inducted by radiation and electrical stress

(iv) perform spectroscopic studies to compare electrically active defects with defects observed spectroscopically

Gerry Thanks You

1 step monoclinic HfO_2

textured epi-growth - independent of acidic or basic

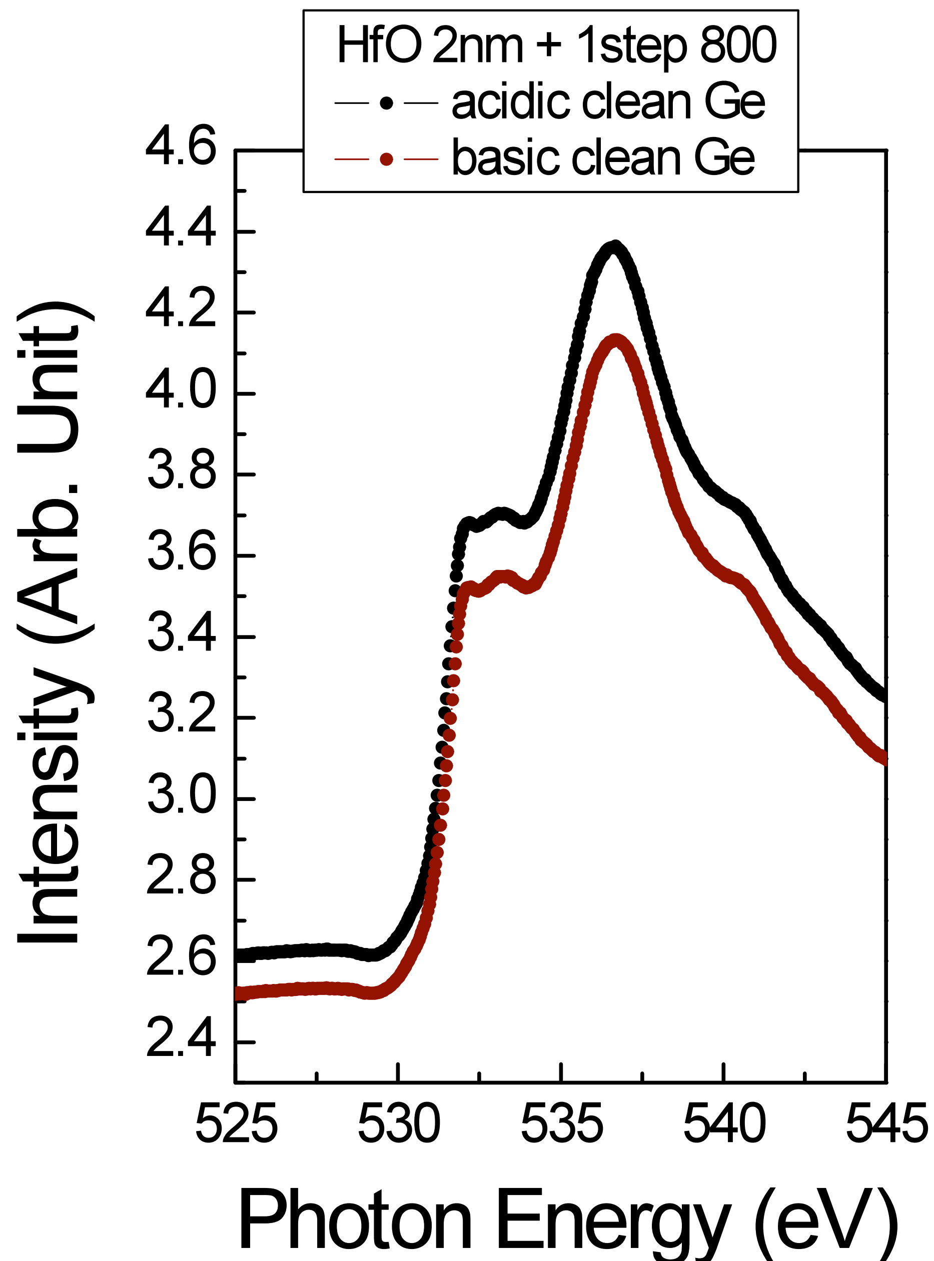

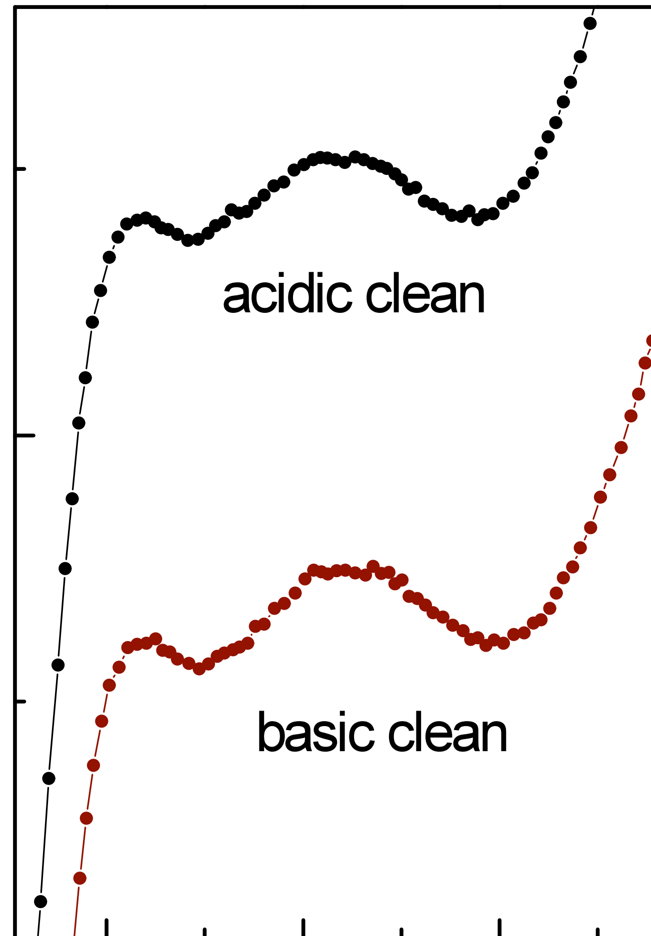

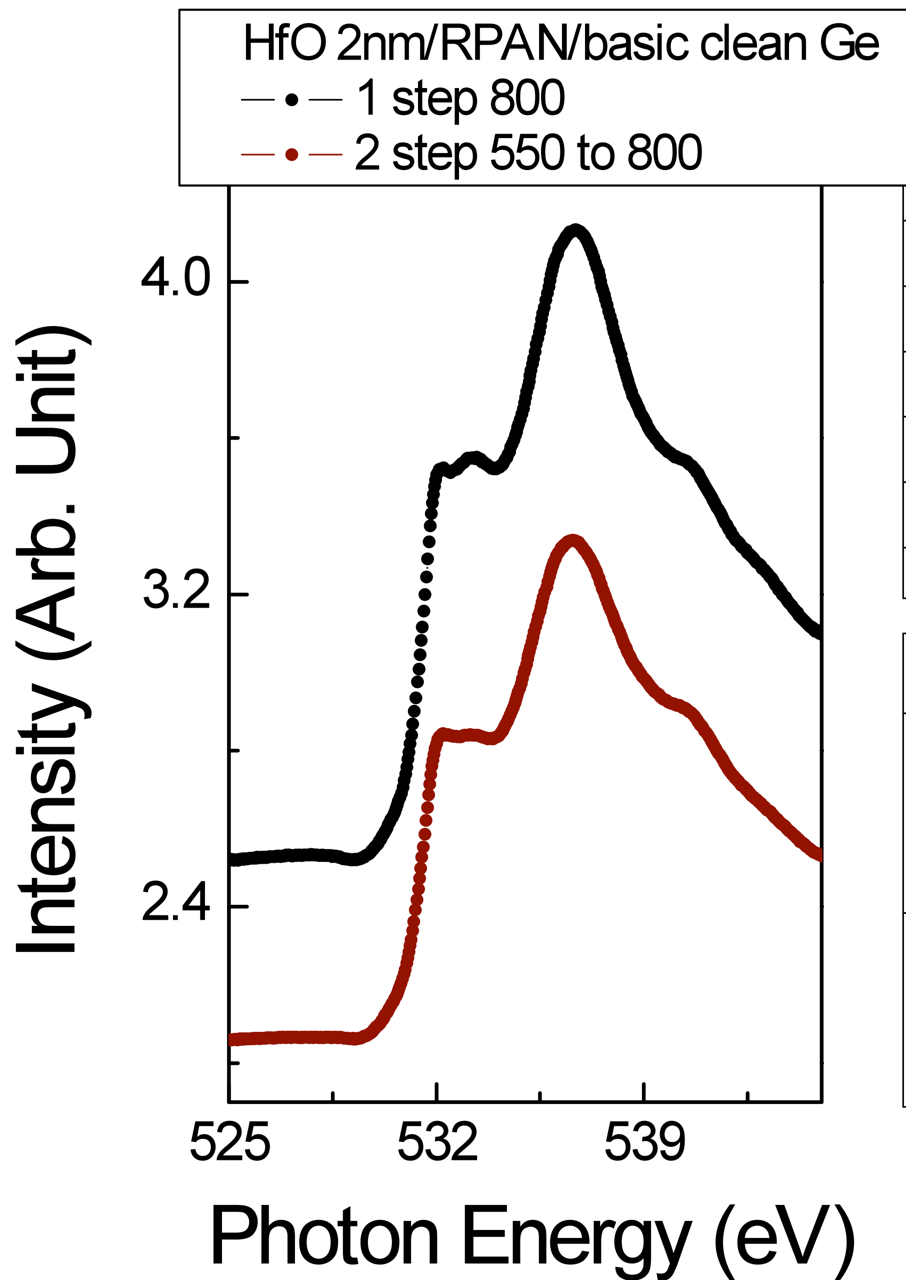

1 step monoclinic HfO_2

textured epi-growth - aligned to dimer rows of Ge(100)

2 step mixed monoclinic-tetrahedral HfO_2 grains

Ge-Hf oxide dielectric at interface after anneal

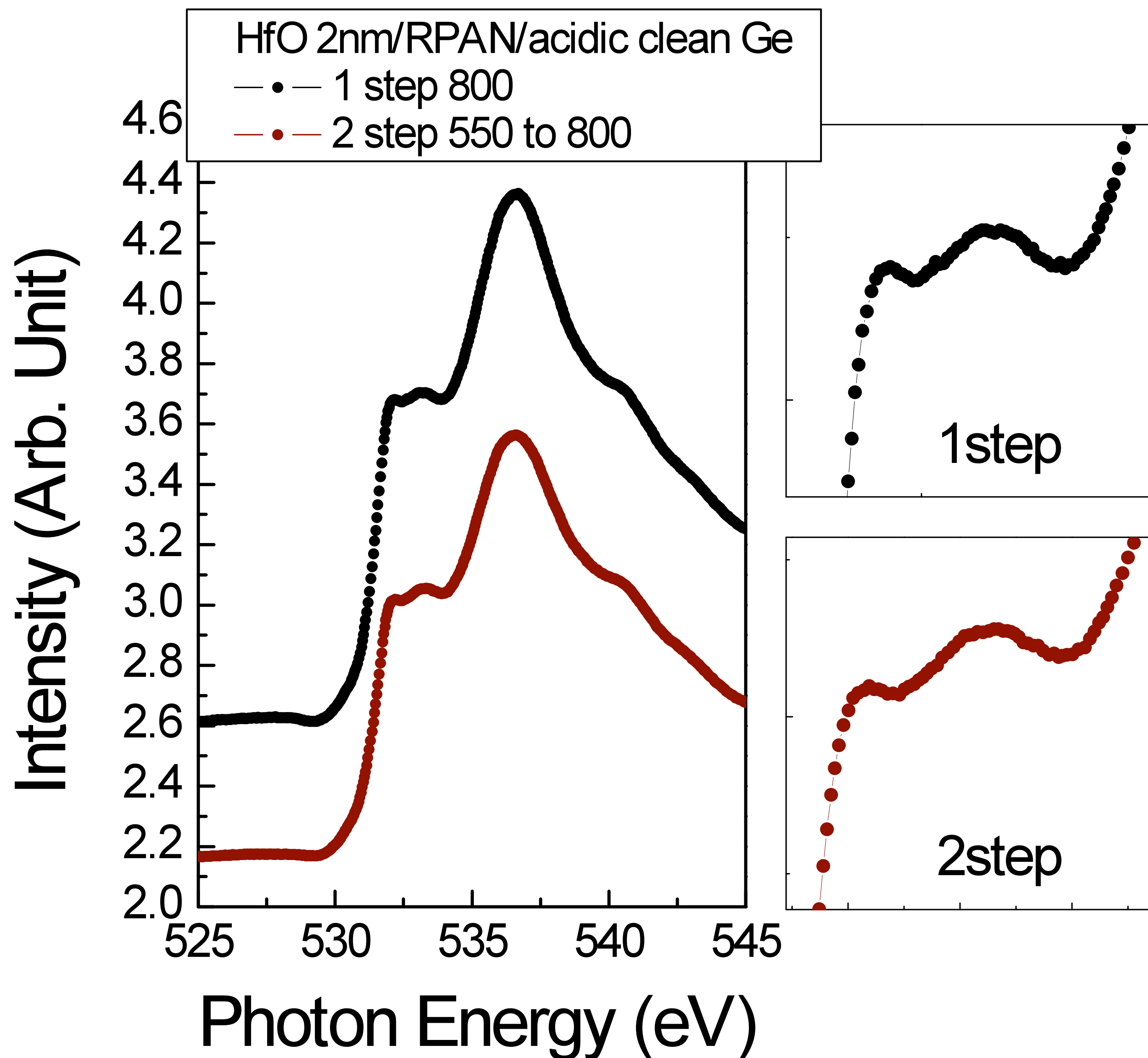

1 step and two step with acidic clean give monoclinic HfO_2

textured epi-growth - aligned to dimer rows of Ge(100)

1 step monoclinic HfO_2

textured epi-growth - independent of acidic or basic

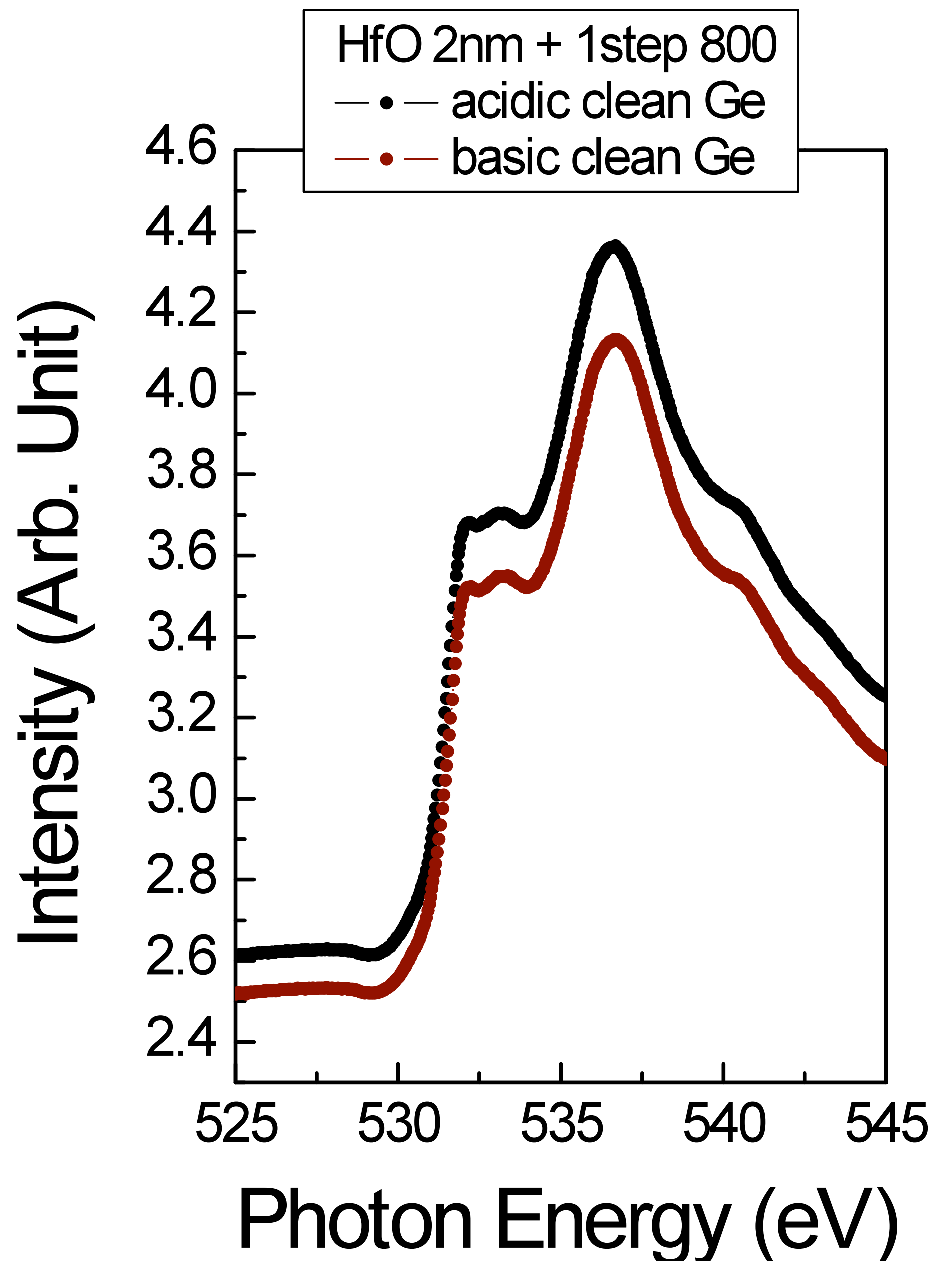

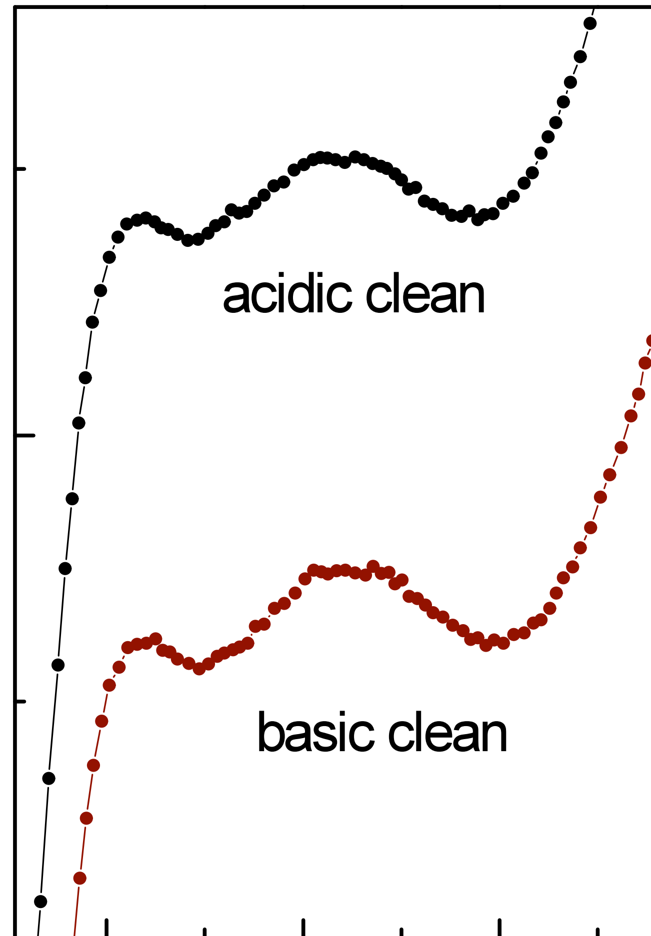

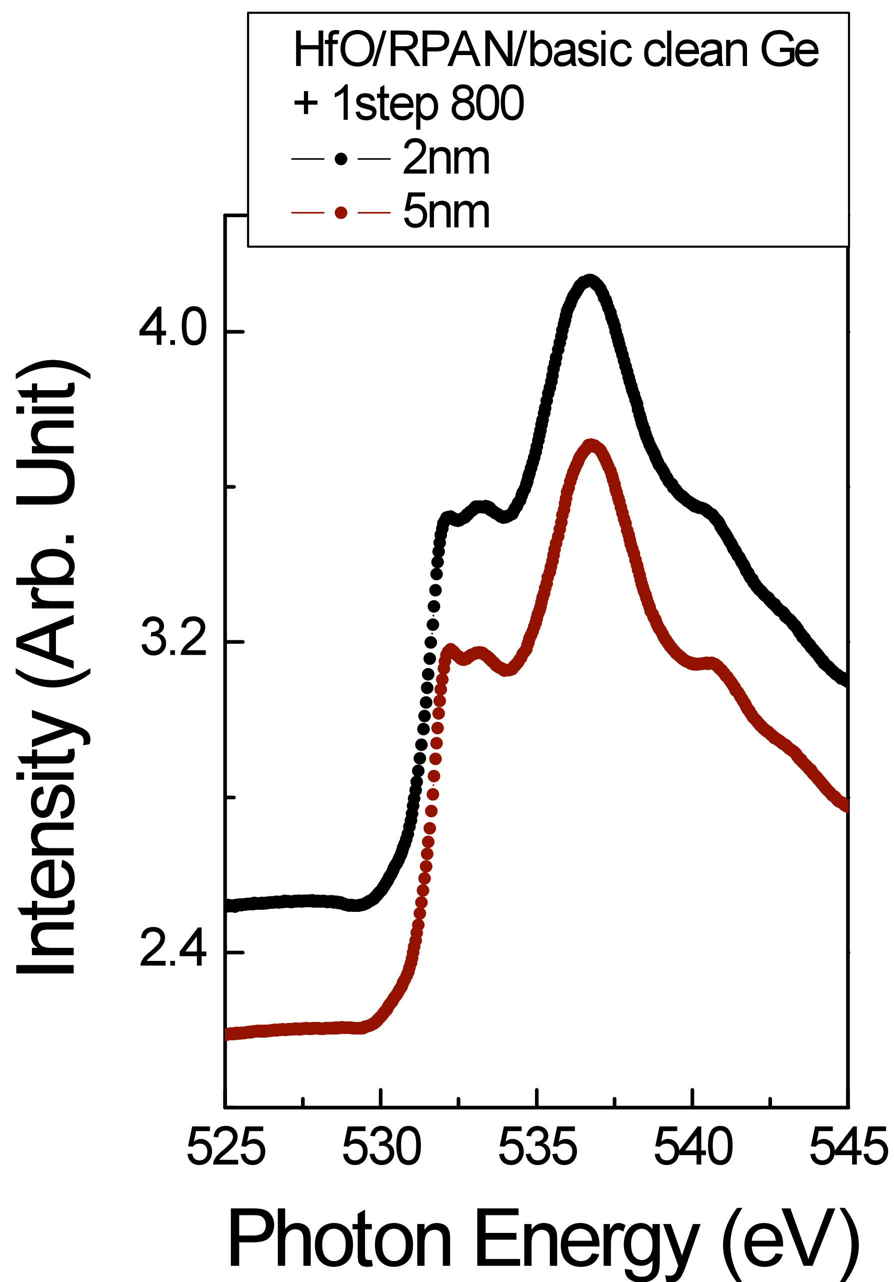

2nm

5nm

2nm 1 step
monoclinic HfO_2

textured epi-growth - aligned to dimer rows of Ge(100)

5nm 1 step
t- HfO_2 on m-HfO_2

as film grows mixed m- and t- grains are formed - growth loses contact with Ge surface geometry

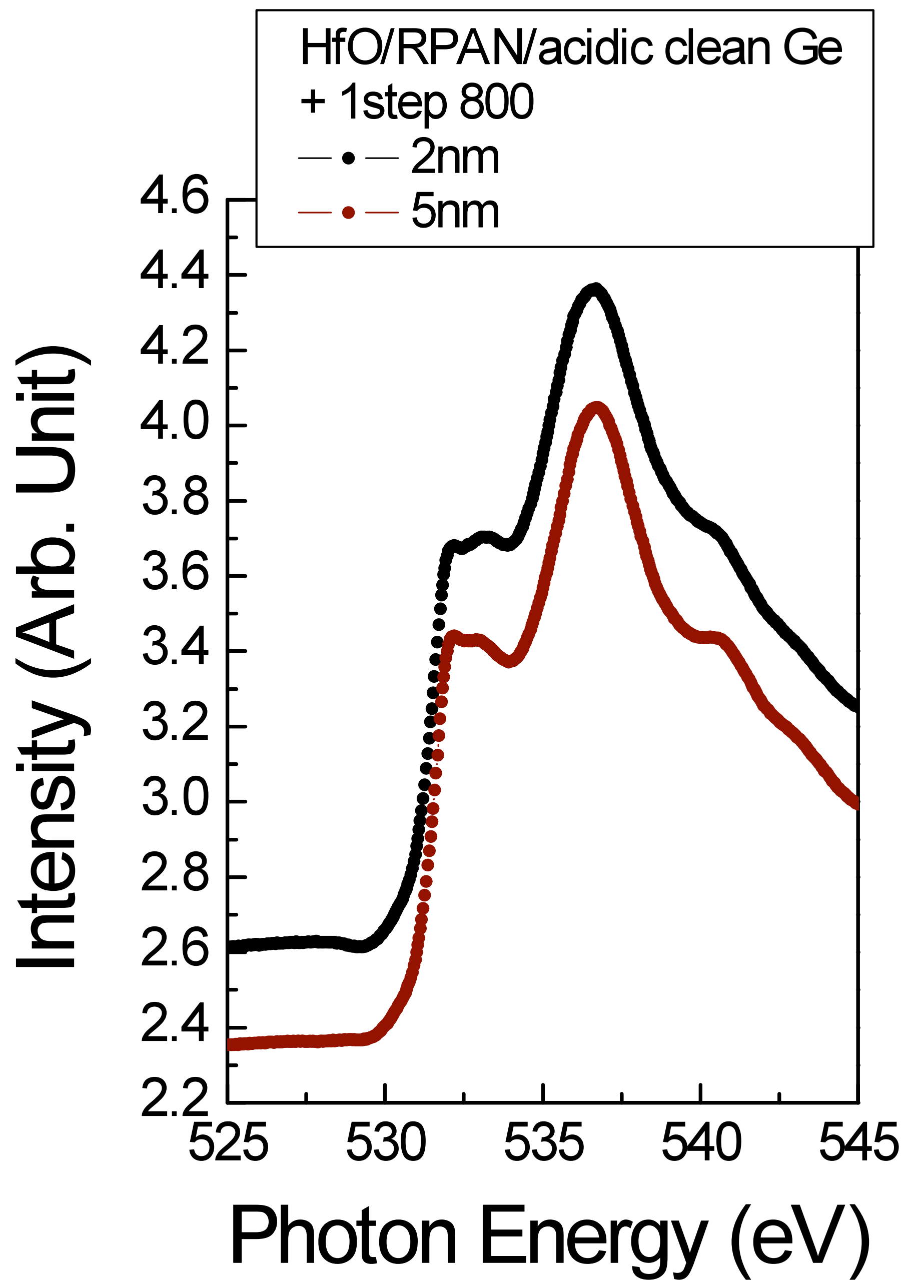

2nm

5nm

2nm 1 step
monoclinic HfO_2

5nm 1 step
t- HfO_2 on m-HfO_2

mixed grain growth
in thicker films
independent of
surface clean

perpendicular and parallel are with respect to wafer flat, and there mean 90 rotation of dimer rows of Ge(001)

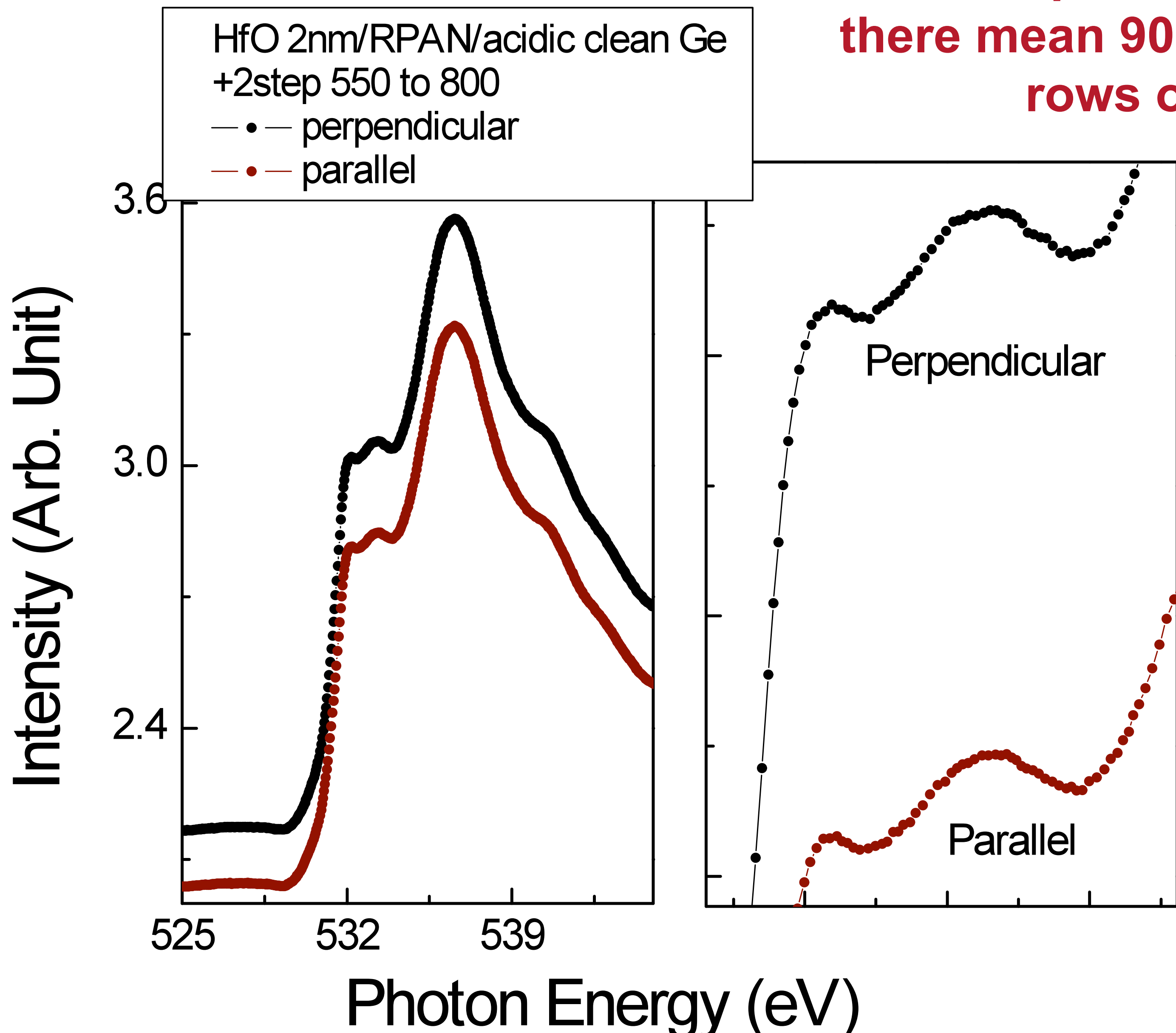

since both spectra are the same - axis of unit cell for alignment makes an angle of 45 degrees with respect to dimmer rows

XAS O K_1 edge: top (a) HfO_2 on Ge-(b) HfSiON on Ge BottomL 2nd derivative O K_1 edge. Gaussian fits: energies 2nd derivatives give, crystal field (C-F) splittings Jahn-Teller (J-T) *d*-state degeneracy removal: molecular orbital labels: local bonding symmetry-group theory.

defect states below the conduction band edge ~ 530 eV from 2nd derivative spectra - Gaussian fits next slide

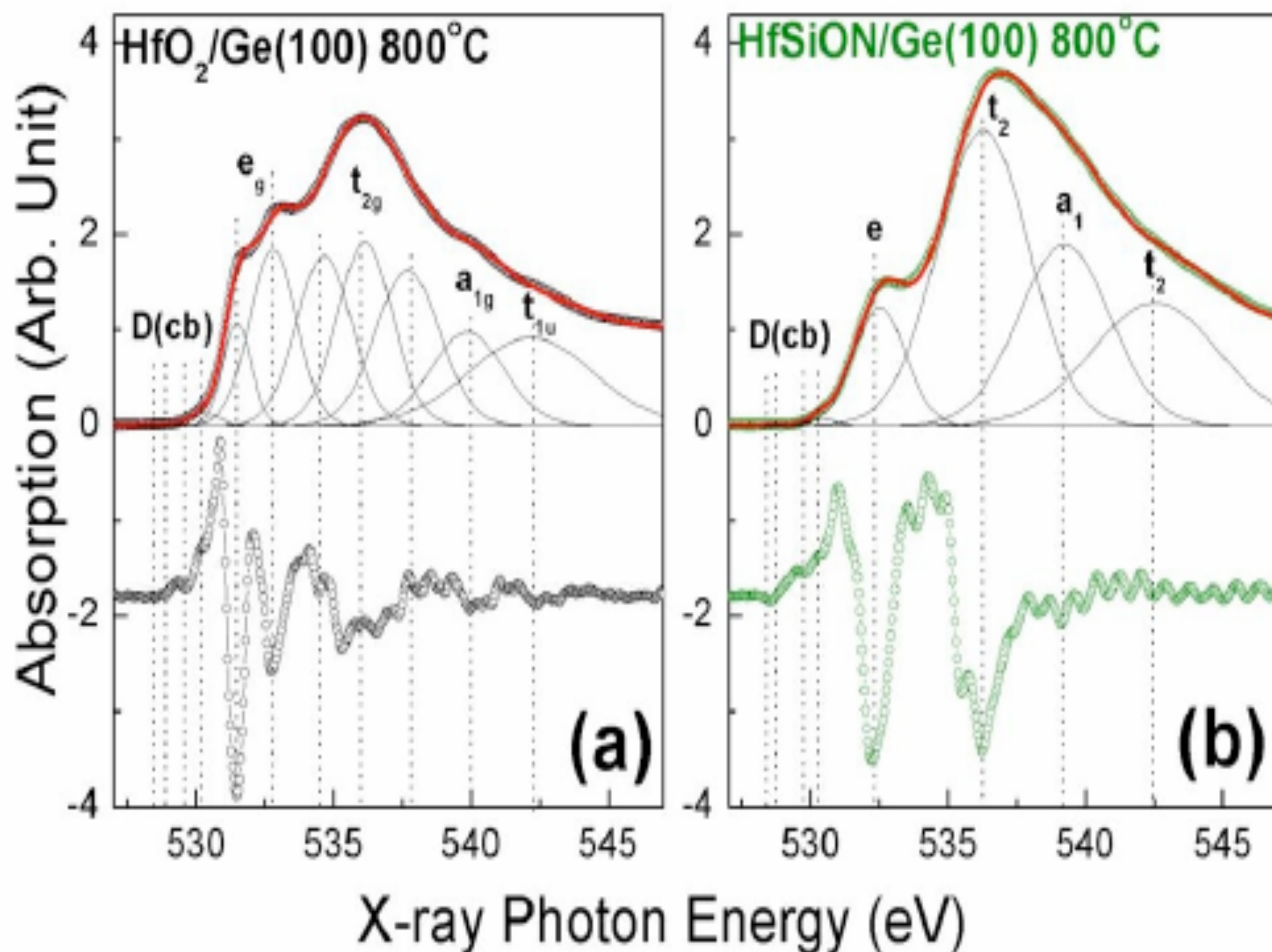

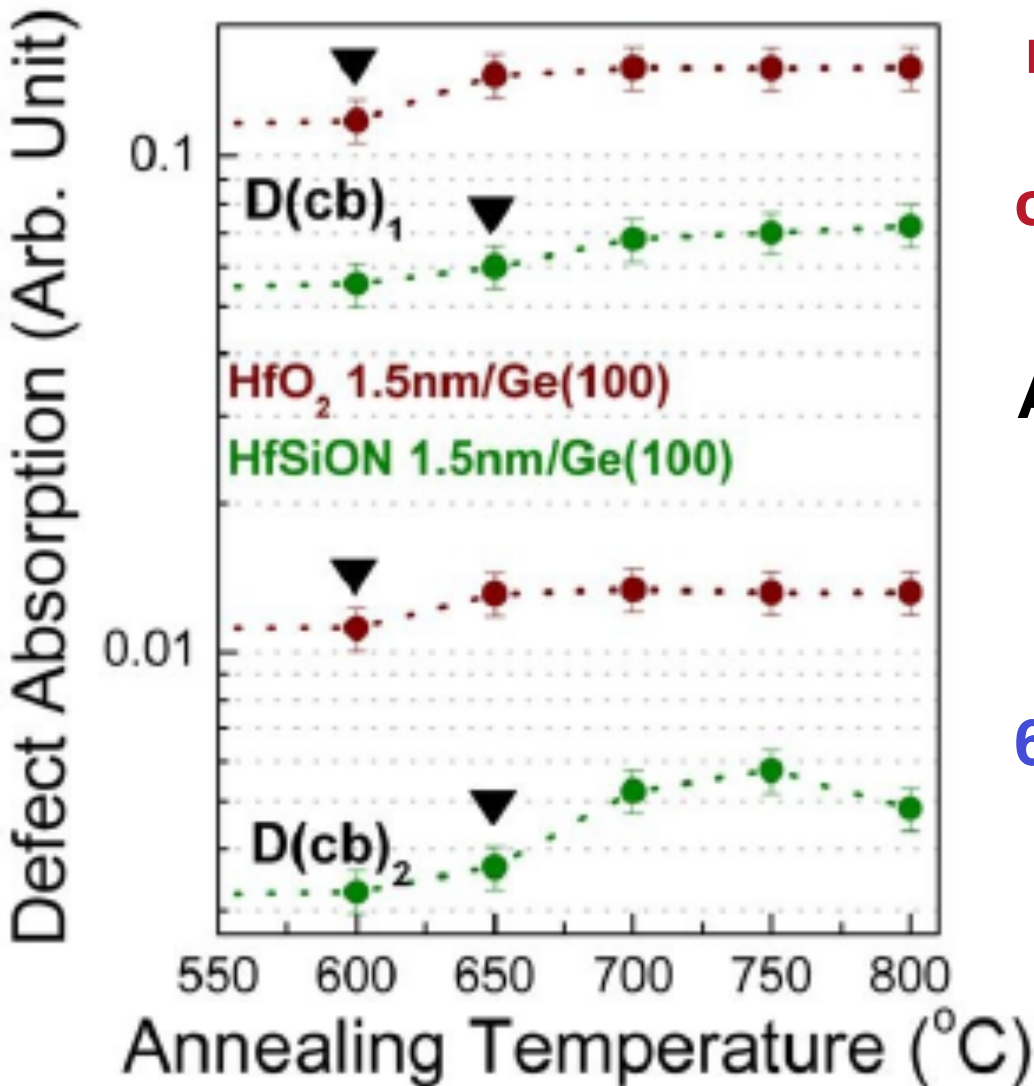

thermal evolution of relative absorption for two distinct defect states, calculated by Gaussian fits in previous slide

Arrows indicate the onsets of distinct changes in theses trends for each defect state.

600-650°C release if N from GeN as observed in N K edge spectra

Differences Between Charge Trapping States in Irradiated Nano-crystalline HfO_2 and Non-crystalline Hf Silicates

G. Lucovsky,[1] S. Lee,[1] H. Seo,[1] R. D. Schrimpf,[2] D. M. Fleetwood,[2] J. A. Felix,[3] J. Luning,[4] L. B. Fleming,[1] M. Ulrich,[1] and D. E. Aspnes[1]

[1]Department of Physics and Electrical and Computer Engineering, North Carolina State University, Raleigh, NC 27695, USA
[2]Department of Electrical Engineering and Computer Science, Vanderbilt University, Nashville, TN 37235, USA
[3]Sandia National Laboratories, Albuquerque, New Mexico 87185-1083, USA
[4]Stanford Synchrotron Radiation Laboratory, Menlo Park, CA 94025, USA

Supported in part by ONR, SRC, and an AFOSR MURI

[3]Sandia is a multiprogram laboratory operated by Sandia Corporation, a Lockheed Martin Company, for the United States Department of Energy's National Nuclear Security Administration under Contract DE-AC04-94AL85000.

Outline

- Experimental results on hole and electron trapping
    - Hf silicate (amorphous)
    - HfO_2 (nano-crystalline)
- New spectroscopic evidence
    - Hf and other group IV B oxides
    - Soft x-ray photoelectron spectroscopy (SXPS)
- Insight into differences into electron and hole trapping
- New promise for advanced high-κ dielectrics

Radiation response of Hf Silicate capacitors

Mostly hole trapping in oxide

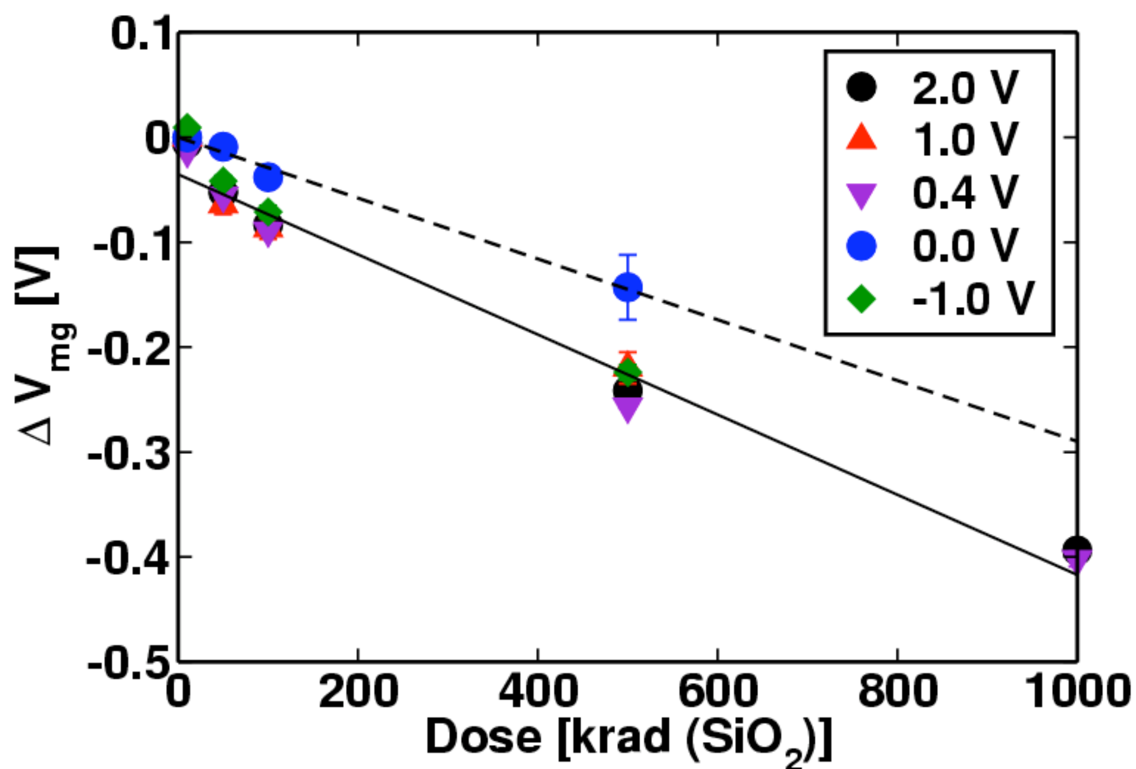

J. A. Felix, D. M. Fleetwood, R. D. Schrimpf, J. G. Hong, G. Lucovsky, J. R. Schwank, and M. R. Shaneyfelt, *IEEE Trans. Nucl. Sci.*, vol. 49, pp. 3191-3196, 2002.

Radiation response of HfO_2 capacitors
Both hole and electron trapping

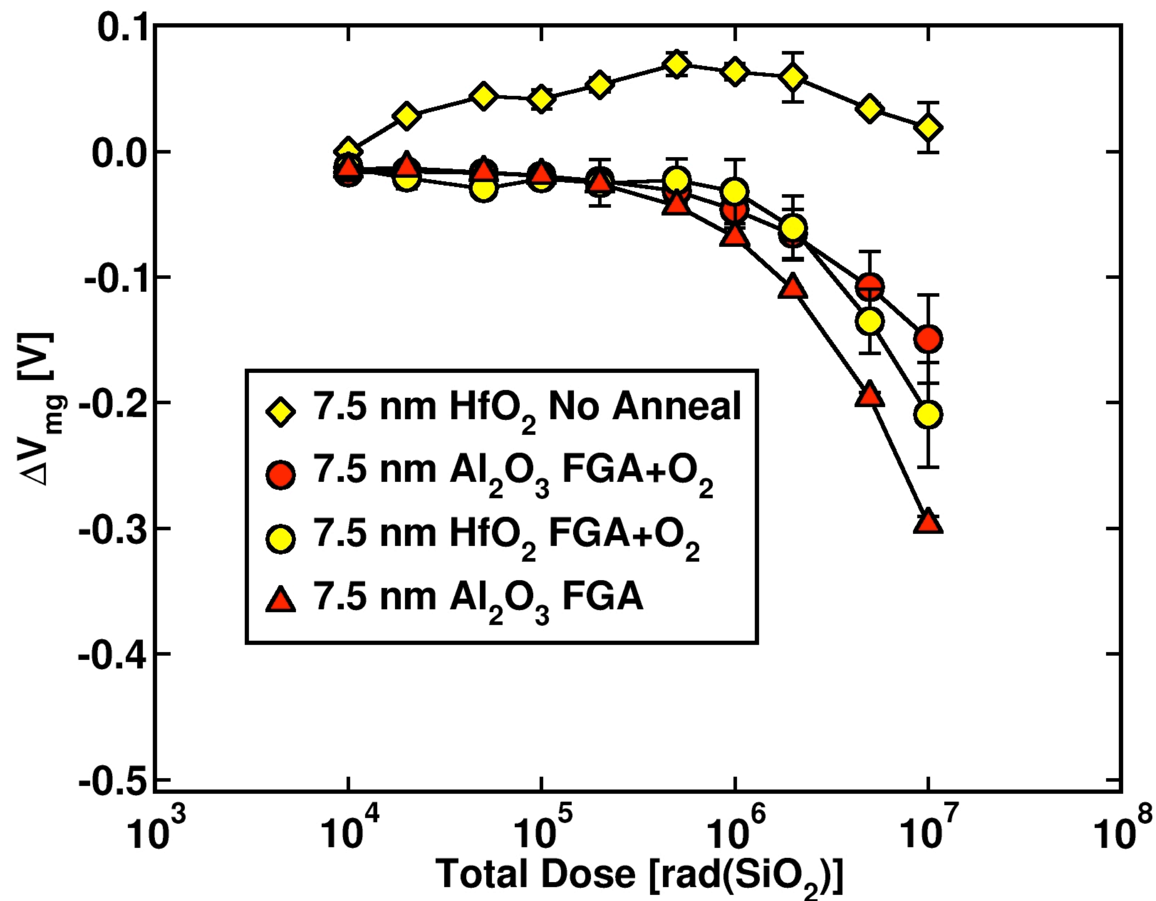

J. A. Felix, J. R. Schwank, D. M. Fleetwood, M. R. Shaneyfelt, and E. P. Gusev, *Microelectron. Reliab.*, vol. 44, pp. 563-575, 2004.

Micro-structure of nano-crystalline HfO_2 and non-crystalline Hf silicates and nitrided Hf silicates

nano-crystalline HfO_2

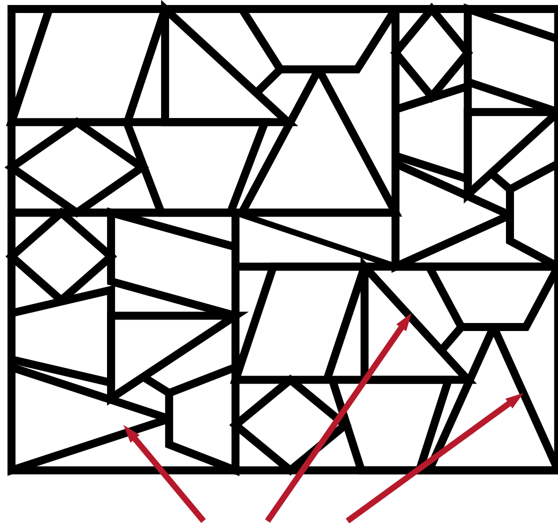

grain boundaries

crystallite size: 2 to 100 nn

grain boundaries - intrinsic bonding defects

local defects at band edges

trap both holes and electrons

amorphous Hf silicate

isotropic and homogeneous

no discernable granularity

band tail states due to random local atomic structure

localized defect states

generally deep in gap

specific bonding defects

broken bonds - chemical impurities

Spectroscopic evidence for band edge defects in HfO_2

Soft x-ray photoelectron spectroscopy (SXPS)

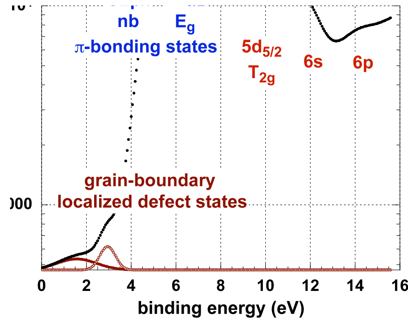

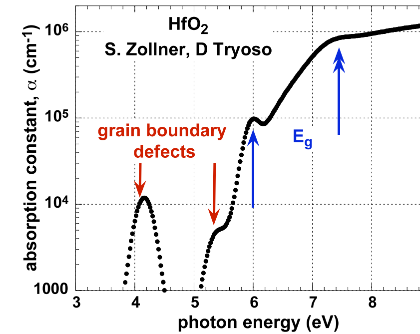

partially-filled defect states at valence band edge

hole or electron traps

empty defect states at conduction band edge

electron traps

Intrinsic band edge defect states function as electron and hole traps in a radiation or high-field stress environment

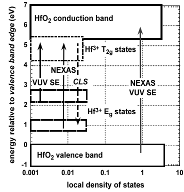

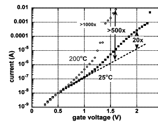

trap-assisted transport of electrons through empty states

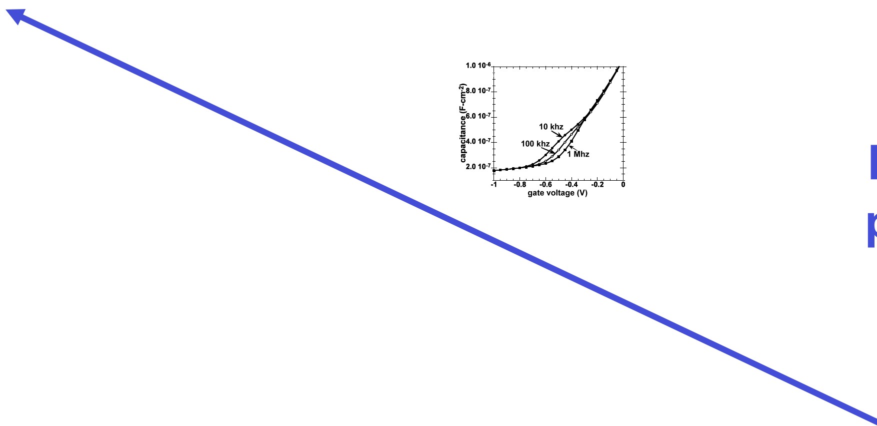

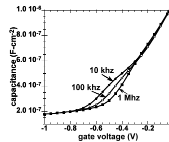

hole trapping into partially-occupied states

Mechanisms during post-rad/CVS NBTS on HfO_2 capacitors

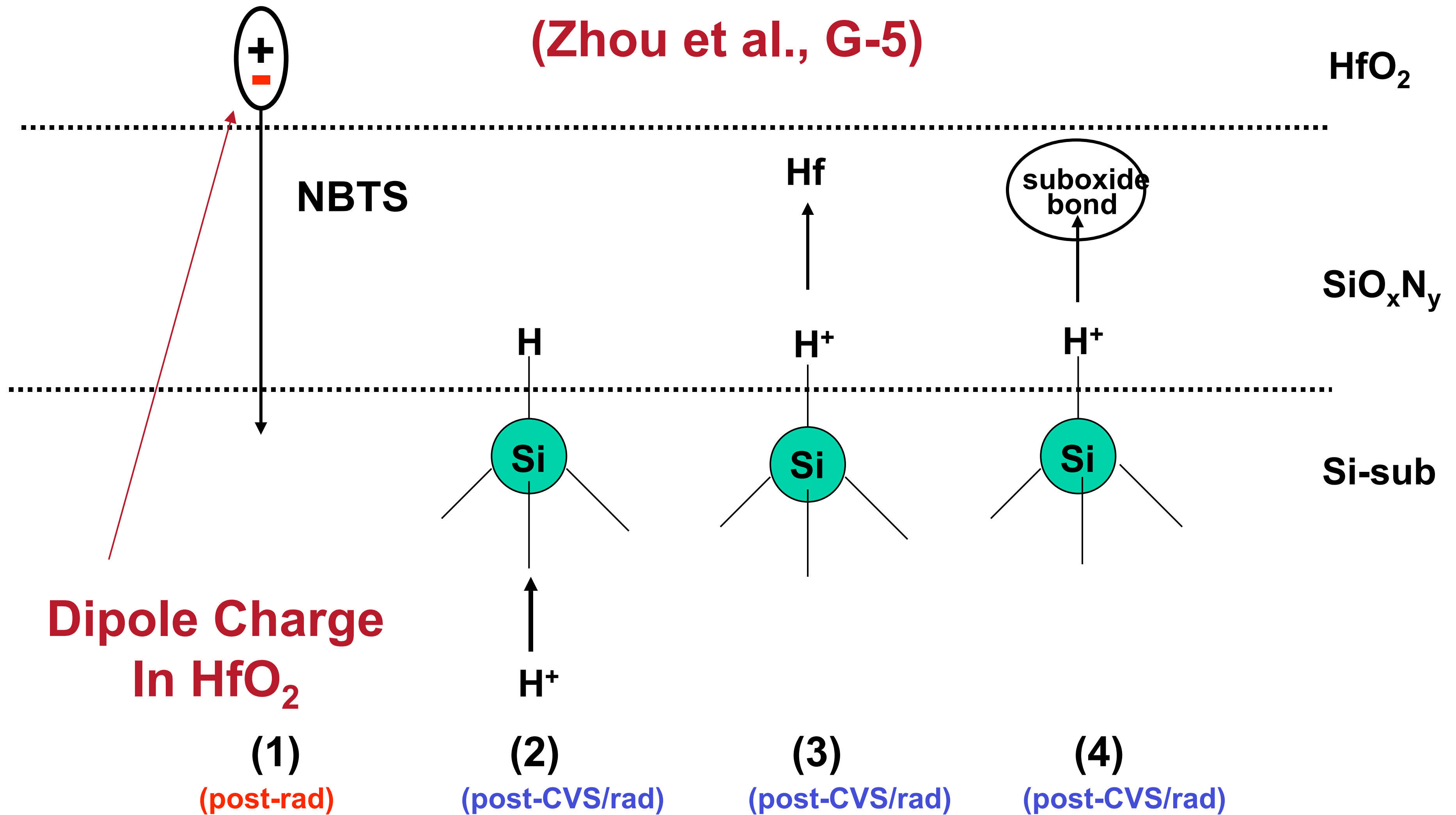

Ultra-thin HfO_2 is a valid engineering solution for advanced devices

band edge states change dramatically
in ultra-thin HfO2 thin films
for ≤ 2 nm physical thickness

no Jahn-Teller effects and no band edge states in SXPS

Sematech, and ST Micro report dramatic drops in defects as well

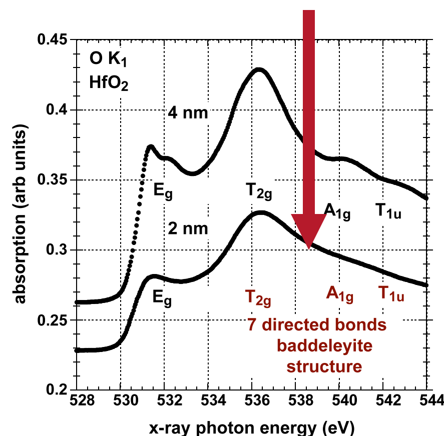

Ultra-thin phase separated 80% HfO_2: almost promising
(nano-crystalline HfO_2 with nano-scale SiO_2 inclusions)

band edge J-T term-splittings suppressed by small sizes (<2 nm) in nano-crystalline grains due to SiO_2 inclusions

2 nm thick spectra same as 2 nm thick HfO_2 on last slide

4 nm thick sample - grains are anisotropic in growth direction -- therefore narrowing of E_g feature

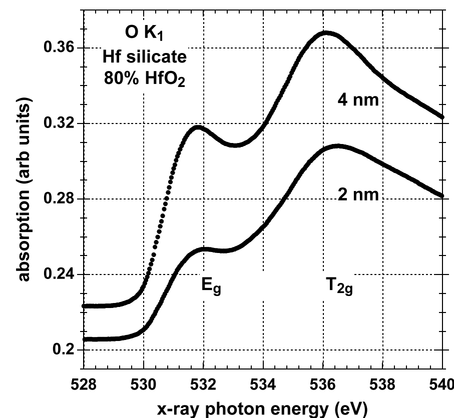

We await results from electrical tests in full devices!

Summary and Conclusions

- Hf silicate and HfO_2 gate dielectrics show differences in electron trapping
- Spectroscopic evidence shows enhanced electron trapping in HfO_2 caused by nano-crystallinity
- Significant issue – especially for combined radiation/reliability response
- New Hf, Zr oxynitrides and thin HfO_2 films (with/without SiO_2 inclusions) may be promising for highly scaled, future technologies
  - Spectroscopic studies show absence of electron traps
  - Await the results of fully processed devices

schematic representation of immobile and mobile vacancy defect bonding

removal to one neutral O-atom - 2 electrons/O in vacancy site

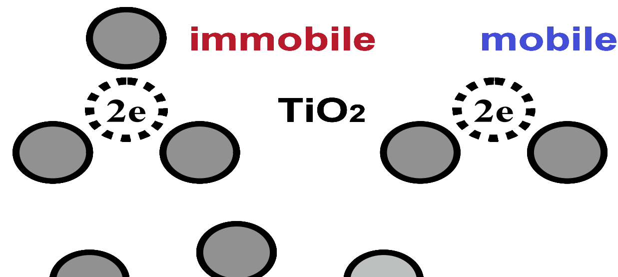

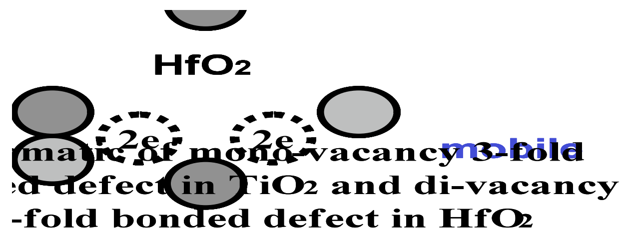

TiO_2 local bonding in distorted rutile geometry -- 6 fold coordinated Ti and 3 fold coordinated O

immobile 3 Ti; mobile 2Ti

HfO_2 local bonding in distorted CaF_2 geometry -- 8 fold coordinated Hf and 4 fold coordinated O

immobile 6 Hf; mobile < 6Hf, e.g., 4 or 5 Hf

mono-vacancy (or simply vacancy) defects

2 states at band edge in SXPS TiO_2 - consistent with d^2 description

XAS pre-edge & virtual bound state regimes - additional confirmation

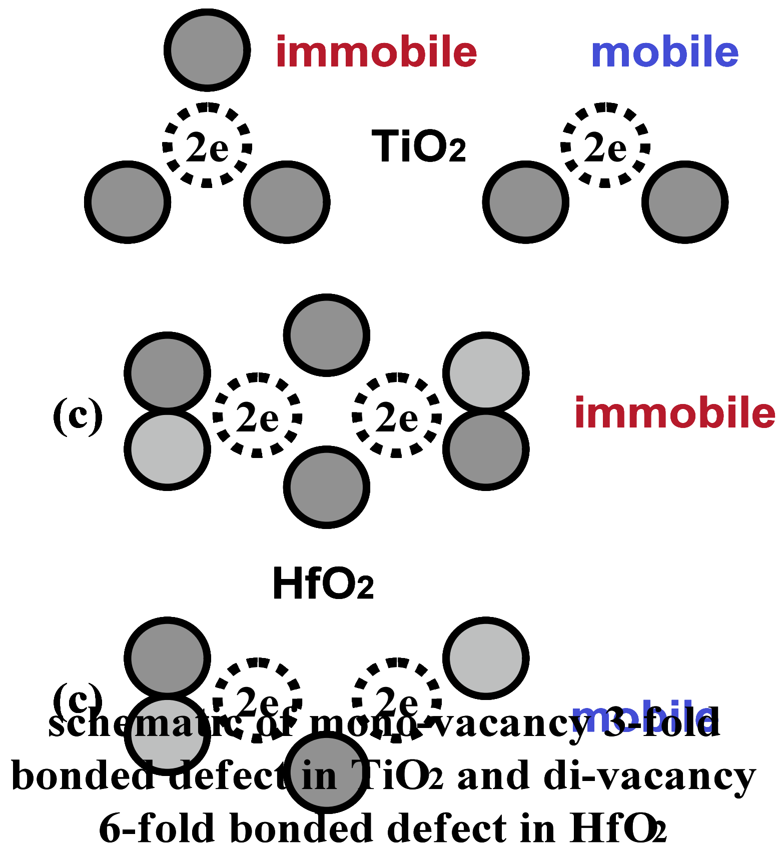

schematic of mono-vacancy 3-fold bonded defect in TiO_2 and di-vacancy 6-fold bonded defect in HfO_2

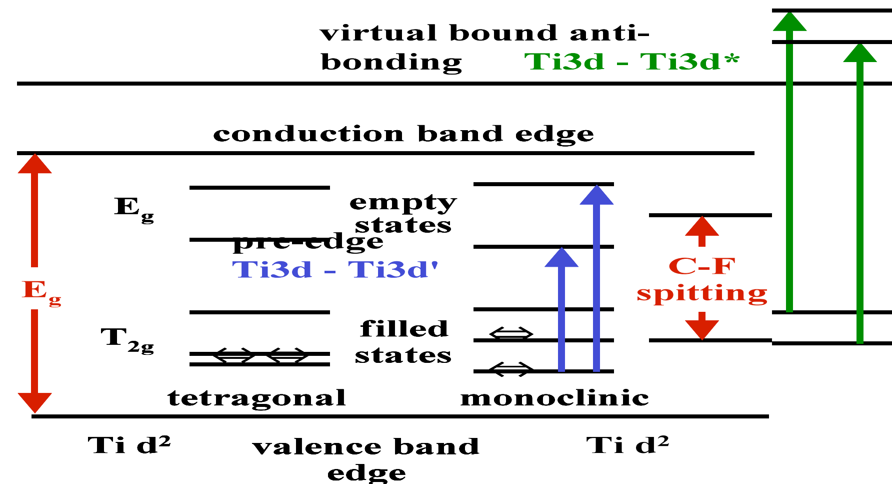

mono-vacancies are d^2 -- di-vacancies are d^4

difference between immobile and mobile - spectral widths proportional to crystal field - number of atoms bordering on defect

summary of d-d' transitions* for HfO_2 d^4 divacancies and TiO_2 d^2 mono-vacancies

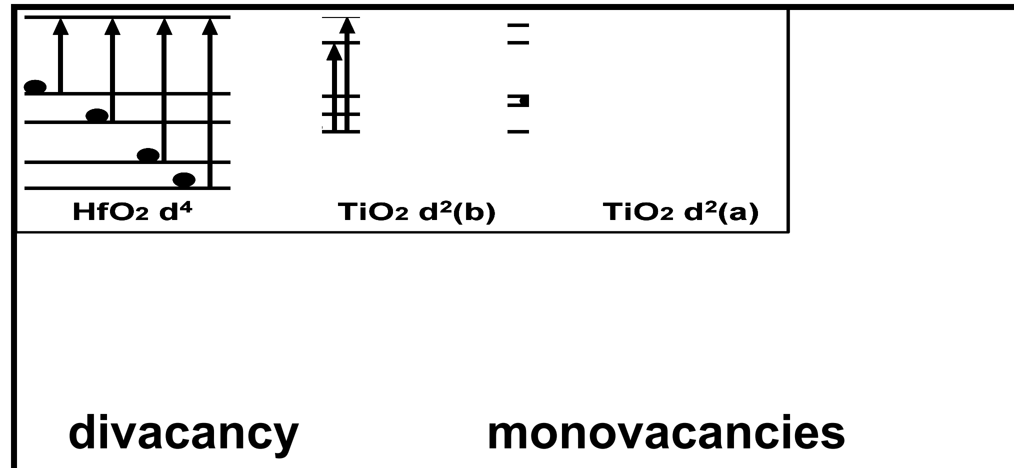

HfO_2 immobile and TiO_2 (a) = mobile and (b) = immobile

***common mistake -- assumption that these transitions originate at top of VB places the final states to deep in the gap (SEMATECH group at WoDiM 2008, and T-J King's group in JVST paper)**

significant issue for interpretation of trap level for trap assisted tunneling and/or PF transport